The Origin of Chemical Shifts

Panacea

June, 16-21 Venice, Italy

Prof. Christophe Copéret
Department of Chemistry and Applied Biosciences
ETH Zürich
ccoperet@ethz.ch
http://www.coperetgroup.ethz.ch/

NMR beyond Numbers

Understanding Electronic Structure and Reactivity from NMR

A journey that started from close discussions with

R.A. Andersen (UC Berkeley)

O. Eisenstein & C. Raynaud (Univ. Montpellier)

and one PhD student

Christopher P. Gordon (ETH Zürich – graduated in 2021)

A story that was supported and continues with:

C. Ehinger, Dr. Z. Berkson, Dr. D. Estes, D. Gioffrè, S. Halbert, Y. Kakiuchi, C. Kaul (**P232**), L. Lätsch, W.-C. Liao, S. Sabisch (**P222**), S. Satoru, Dr. K. Searles, Dr. A. Yakimov, K. Yamamoto…

within collaborations with many more colleagues and friends:
Barnes (ETHZ), Conley (UC Riverside), Fürstner (MPI), Jeschke&Klöse (ETHZ), Kovalenko (ETHZ), Lesage&Pintacuda (C-RMN), Monteil-Raynaud (Univ Lyon), Roman-Leszkov (MIT), Rossini (Iowa), Sigman (Utah), Tamm (Braunschweig), Togni (ETHZ)…as well as Bruker (Hassan/Perrone)

Today's menu, challenges and directions:

- Using NMR Chemical Shift to Probe Electronic Structures and Reactivity

NMR beyond Numbers

Understanding Electronic Structure and Reactivity from NMR

Trends in Carbon-13 Chemical Shift Across Molecules

Organic Compounds

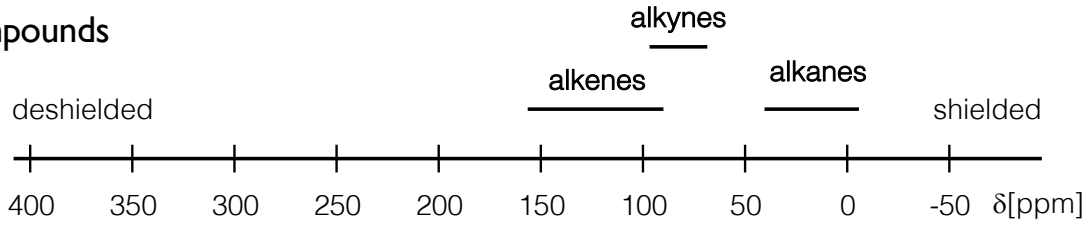

Organometallic Compounds

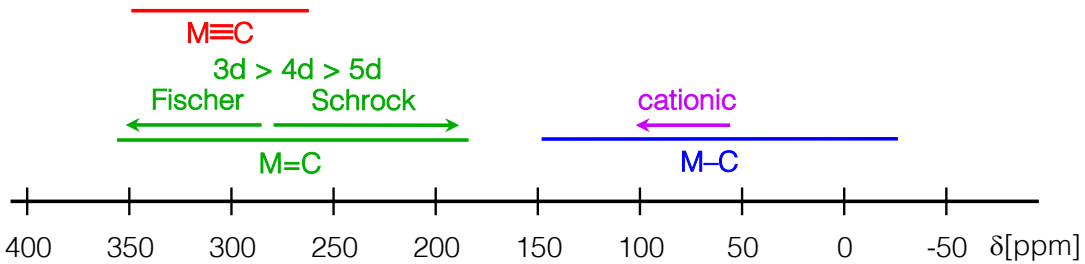

Metal Alkyl

Metal Alkylidene

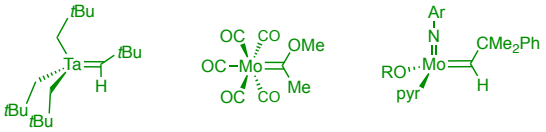

Metal Alkylidyne

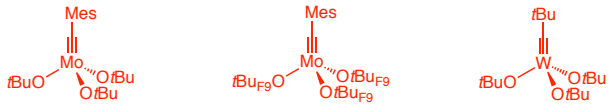

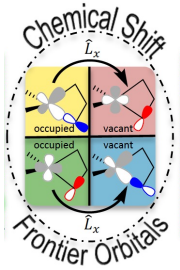

NMR beyond Numbers

Understanding Electronic Structure and Reactivity from NMR

What is Chemical Shift?

Solution (or fast magic angle spinning):
Isotropic Chemical Shift (δ_{iso})

$$\delta_{iso} = \frac{1}{3}(\delta_{11} + \delta_{22} + \delta_{33})$$

$\delta_{11} \geq \delta_{22} \geq \delta_{33}$ $\quad$ $\sigma_{11} \leq \sigma_{22} \leq \sigma_{33}$

$$\begin{pmatrix} \delta_{11} & 0 & 0 \\ 0 & \delta_{22} & 0 \\ 0 & 0 & \delta_{33} \end{pmatrix} = \sigma_{iso}^{ref} \begin{pmatrix} 1 & 0 & 0 \\ 0 & 1 & 0 \\ 0 & 0 & 1 \end{pmatrix} - \begin{pmatrix} \sigma_{11} & 0 & 0 \\ 0 & \sigma_{22} & 0 \\ 0 & 0 & \sigma_{33} \end{pmatrix}$$

See Malcolm Levitt's Presentation

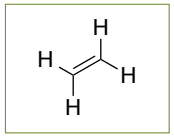

solution

Solid State (static or slow magic angle spinning):
Chemical Shift and Chemical Shielding Tensors

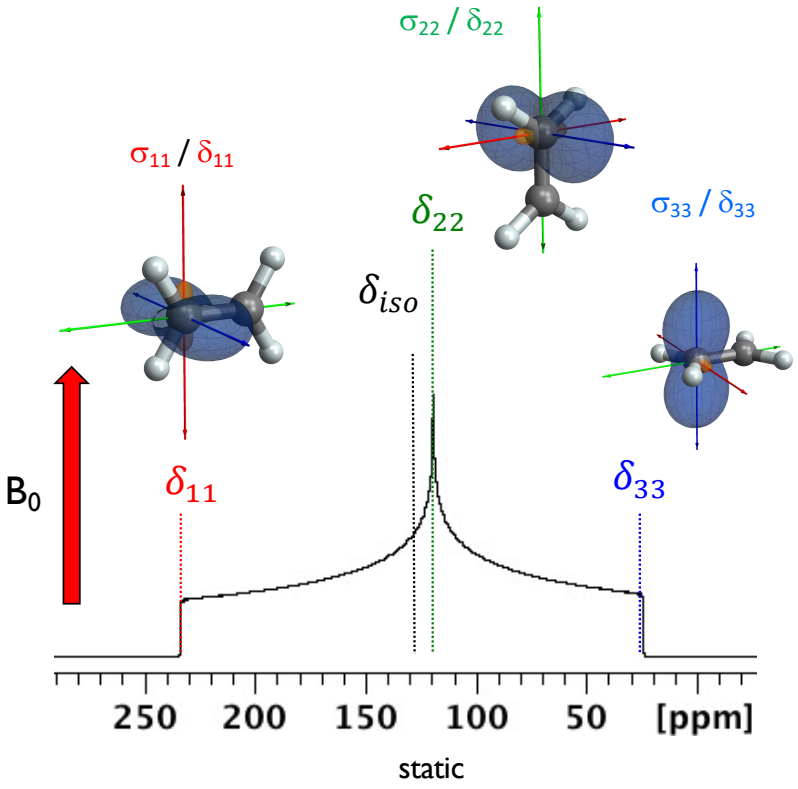

static

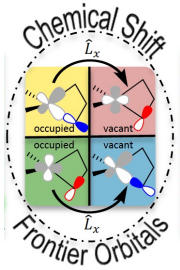

Autschbach, Zheng, and Schurko *Concepts Magn. Reson., Part A* 2010, *361*, 84.
Copéret *et al. J. Am. Chem. Soc.* 2017, *139*, 10588 (Perspectives).
See also: pioneering work of K. Zilm (1980's), A. Pines (1970's)…

NMR beyond Numbers

Understanding Electronic Structure and Reactivity from NMR

What is Chemical Shift?

Solution (or fast magic angle spinning): Isotropic Chemical Shift (δ_{iso})

$$\delta_{iso} = \frac{1}{3}(\delta_{11} + \delta_{22} + \delta_{33})$$

$\delta_{11} \geq \delta_{22} \geq \delta_{33}$ $\quad$ $\sigma_{11} \leq \sigma_{22} \leq \sigma_{33}$

$$\begin{pmatrix} \delta_{11} & 0 & 0 \\ 0 & \delta_{22} & 0 \\ 0 & 0 & \delta_{33} \end{pmatrix} = \sigma_{iso}^{ref} \begin{pmatrix} 1 & 0 & 0 \\ 0 & 1 & 0 \\ 0 & 0 & 1 \end{pmatrix} - \begin{pmatrix} \sigma_{11} & 0 & 0 \\ 0 & \sigma_{22} & 0 \\ 0 & 0 & \sigma_{33} \end{pmatrix}$$

Herzfeld-Berger Convention*

Span $\Omega = \delta_{11} - \delta_{33}$ $\quad$ $(\Omega > 0)$

Skew $\kappa = 3(\delta_{22}-\delta_{iso})/\Omega$ $\quad$ $(-1 \leq \kappa \leq +1)$

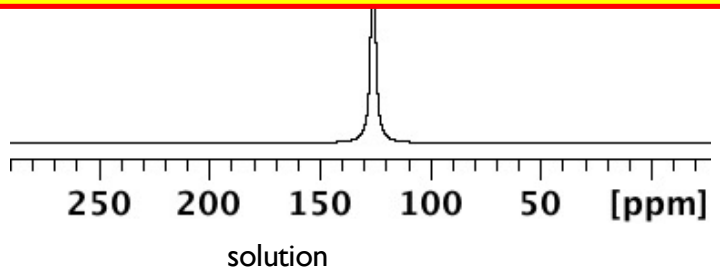

solution

Solid State (static or slow magic angle spinning): Chemical Shift and Chemical Shielding Tensors

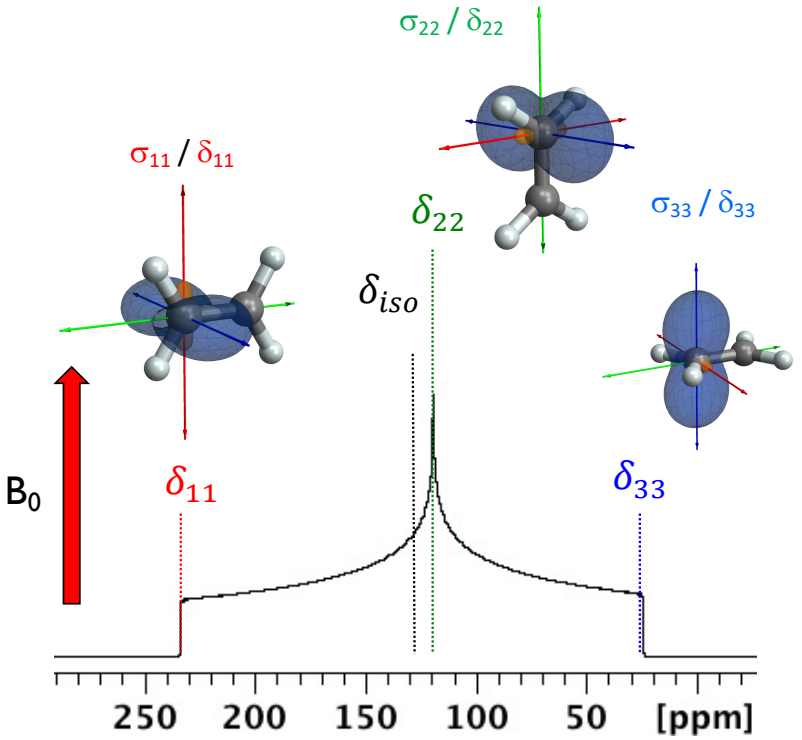

static

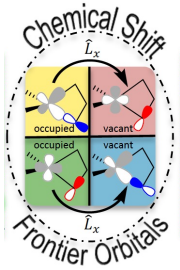

Autschbach, Zheng, and Schurko *Concepts Magn. Reson., Part A* 2010, *361*, 84.

Copéret *et al. J. Am. Chem. Soc.* 2017, *139*, 10588 (Perspectives).

*http://anorganik.uni-tuebingen.de/klaus/nmr/index.php?p=conventions/csa/csa

NMR beyond Numbers

Understanding Electronic Structure and Reactivity from NMR

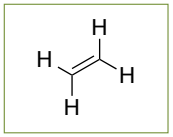

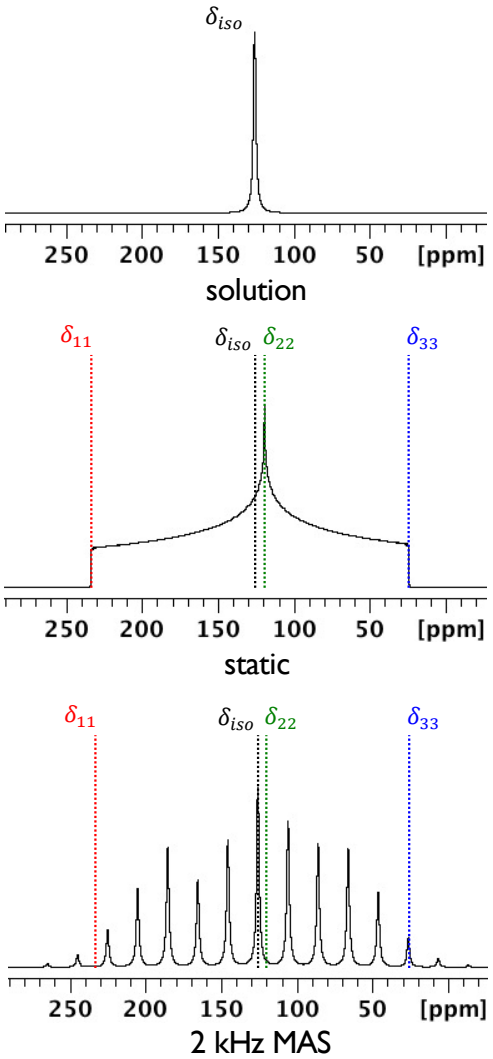

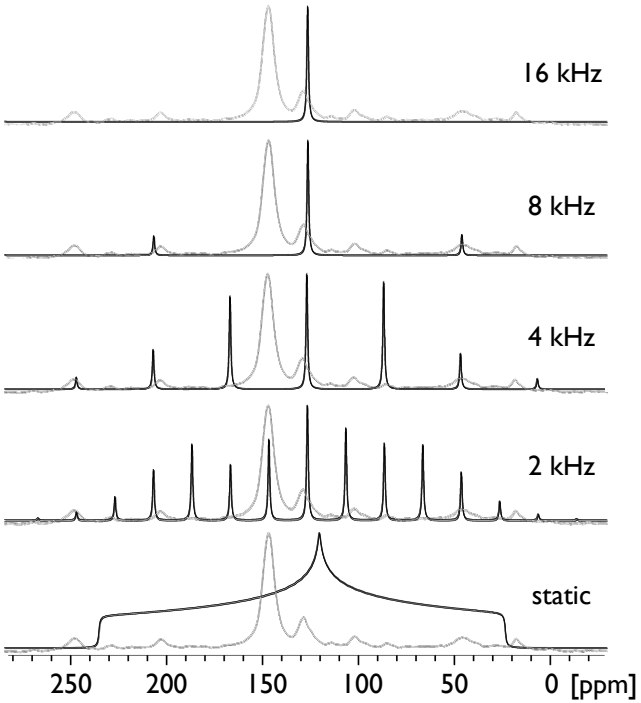

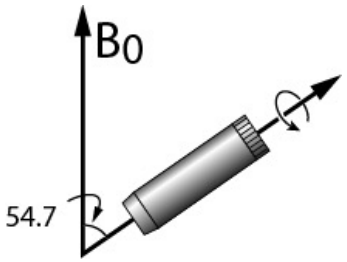

If the sample is spun at a rate less than the magnitude of the anisotropic interaction, a manifold of spinning side bands becomes visible, and they are separated by the rate of the spinning in Hz.

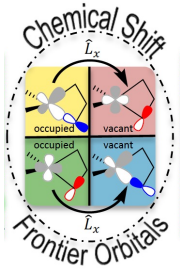

See Malcolm Levitt's Presentation Slide extracted from Lyndon Emsley Lecture Notes

NMR beyond Numbers

Understanding Electronic Structure and Reactivity from NMR

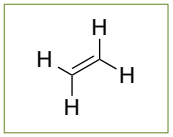

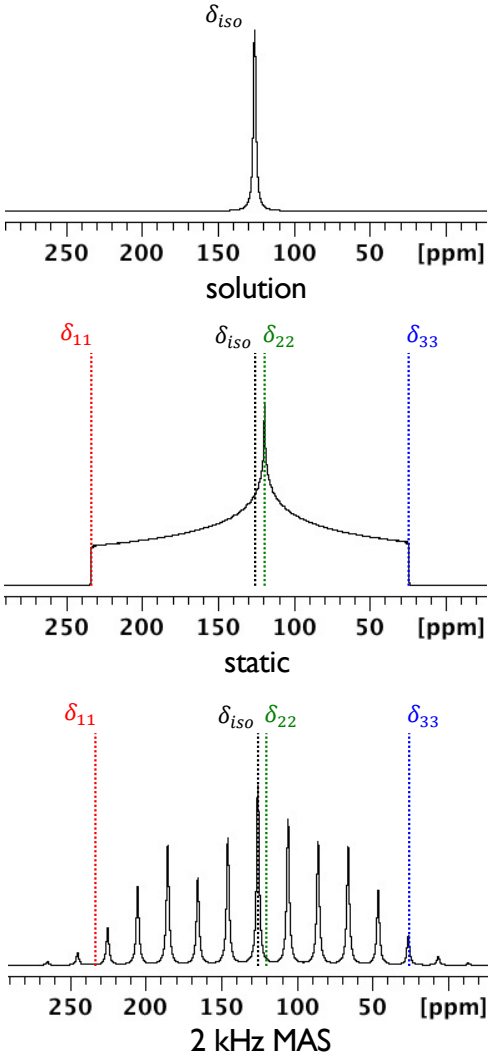

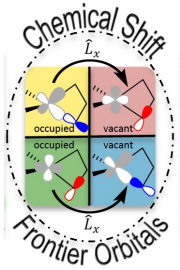

From tensors to electronic structures

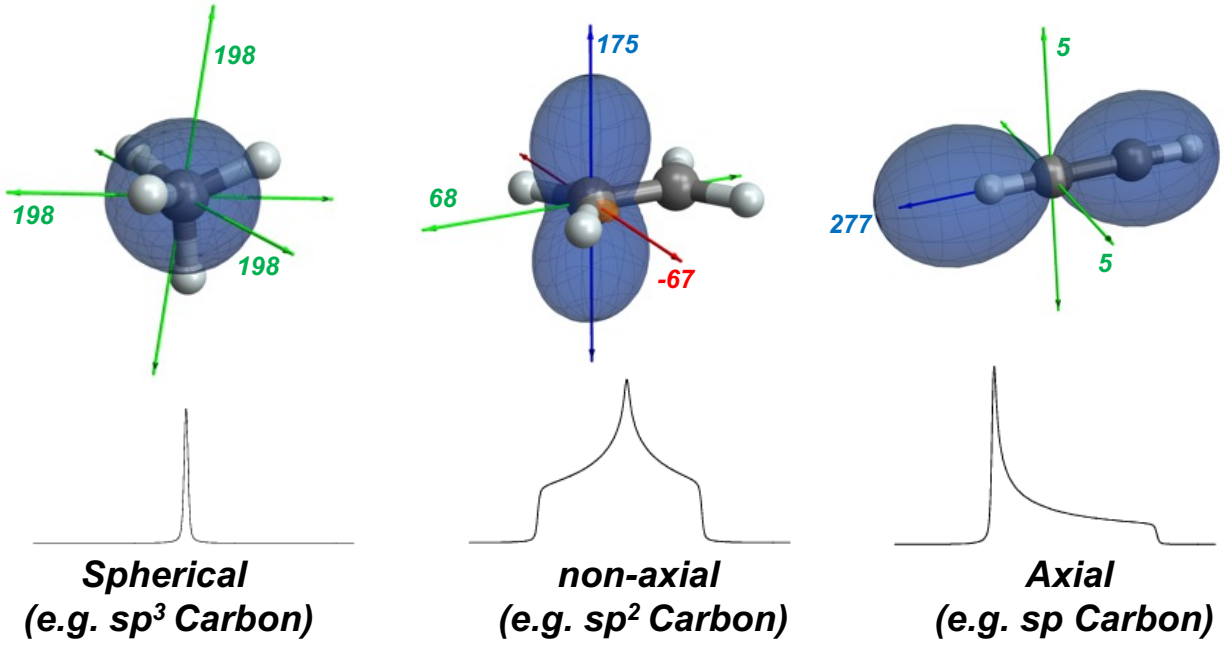

Spherical (e.g. sp^3 Carbon) ***non-axial (e.g. sp^2 Carbon)*** ***Axial (e.g. sp Carbon)***

Autschbach, Zheng, and Schurko Concepts Magn. Reson., Part A 2010, 361, 84.
Copéret et al. J. Am. Chem. Soc. 2017, 139, 10588 (Perspectives).

Chemical Shift vs. Chemical Shielding

Relation of chemical shift (δ) to shielding (σ) with $\delta_{11} > \delta_{22} > \delta_{33}$ (or $\sigma_{11} < \sigma_{22} < \sigma_{33}$)

$$\begin{pmatrix} \delta_{11} & 0 & 0 \\ 0 & \delta_{22} & 0 \\ 0 & 0 & \delta_{33} \end{pmatrix} = \sigma_{iso}^{ref} \begin{pmatrix} 1 & 0 & 0 \\ 0 & 1 & 0 \\ 0 & 0 & 1 \end{pmatrix} - \begin{pmatrix} \sigma_{11} & 0 & 0 \\ 0 & \sigma_{22} & 0 \\ 0 & 0 & \sigma_{33} \end{pmatrix}$$

Decomposition of Chemical Shielding

Decomposition into diamagnetic and paramagnetic terms

$$\sigma = \sigma_{dia} + \sigma_{para+SO} \quad \text{with} \quad \sigma_{ii,para} \Leftrightarrow \frac{\langle \Psi_{vac} | \hat{L}_i | \Psi_{occ} \rangle \langle \Psi_{vac} | \hat{L}_i / r^3 | \Psi_{occ} \rangle}{\Delta E_{vac-occ}}$$

See Jennifer Mathies's Presentation

Origin of Paramagnetic shielding

Pictorial view of coupling between occupied and vacant orbitals, causing deshielding:

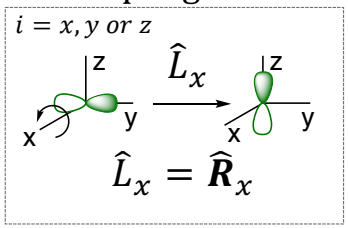

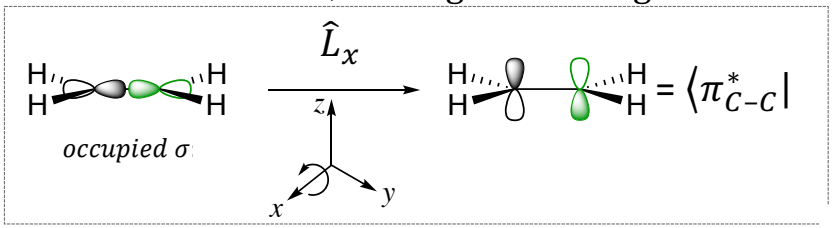

$\hat{R}_x$:Rotational Operator (Group Theory)

$\hat{L}_x |\sigma_{C-C}\rangle =$ 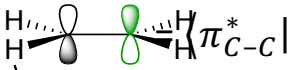 $\langle \pi^*_{C-C} |$

$\langle \pi^*_{C-C} | \hat{L}_x | \sigma_{C-C} \rangle = 1$

σ_{11} / δ_{11}

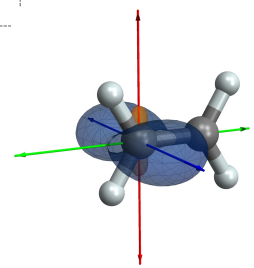

Strong paramagnetic shift for small $\Delta E_{\pi^*-\sigma}$

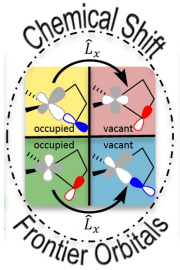

Calculation of NMR and EPR Parameters: Theory and Applications
Prof. Dr. Martin Kaupp, Dr. Michael Bühl, Dr. Vladimir G. Malkin DrSc. Wiley-VCH Verlag, 2004

NMR beyond Numbers

Understanding Electronic Structure and Reactivity from NMR

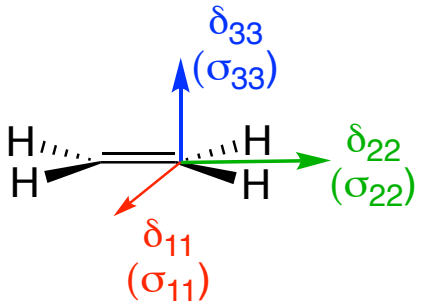

δ_{iso} = 126 ppm

δ_{11} = 234 ppm
δ_{22} = 120 ppm
δ_{33} = 24 ppm

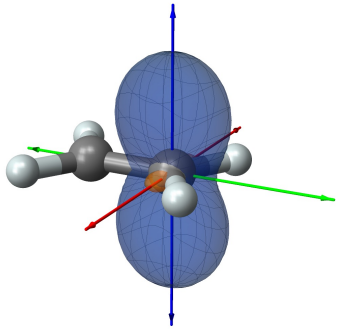

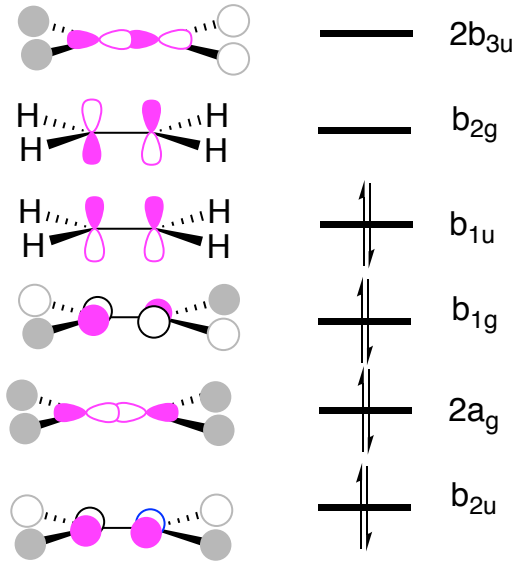

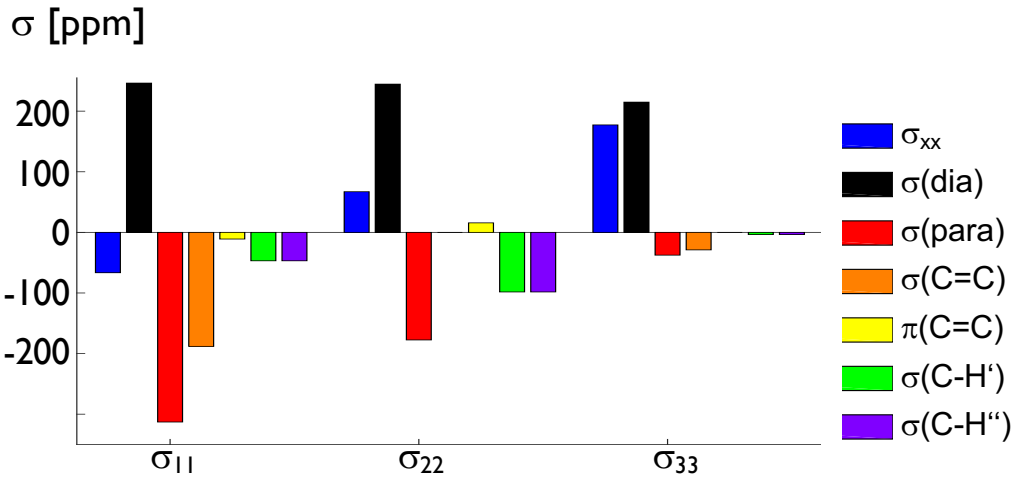

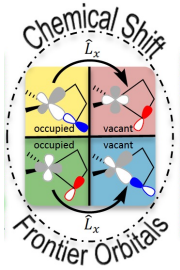

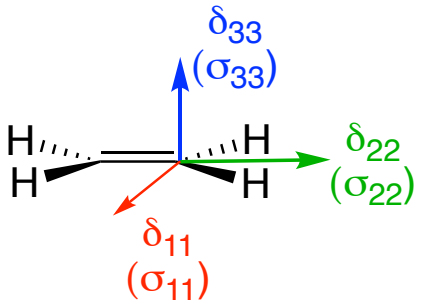

δ_{iso} = 126 ppm

δ_{11} = 234 ppm
δ_{22} = 120 ppm
δ_{33} = 24 ppm

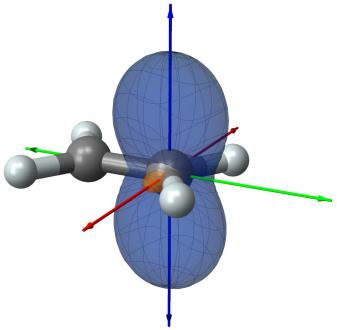

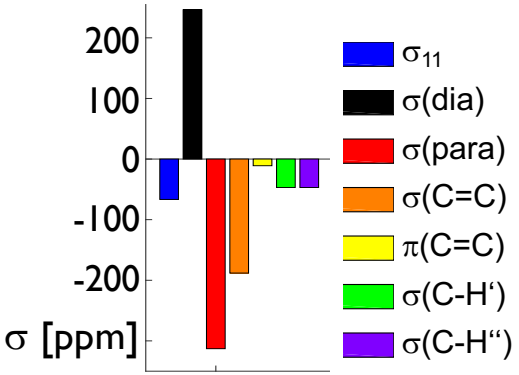

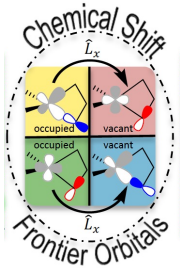

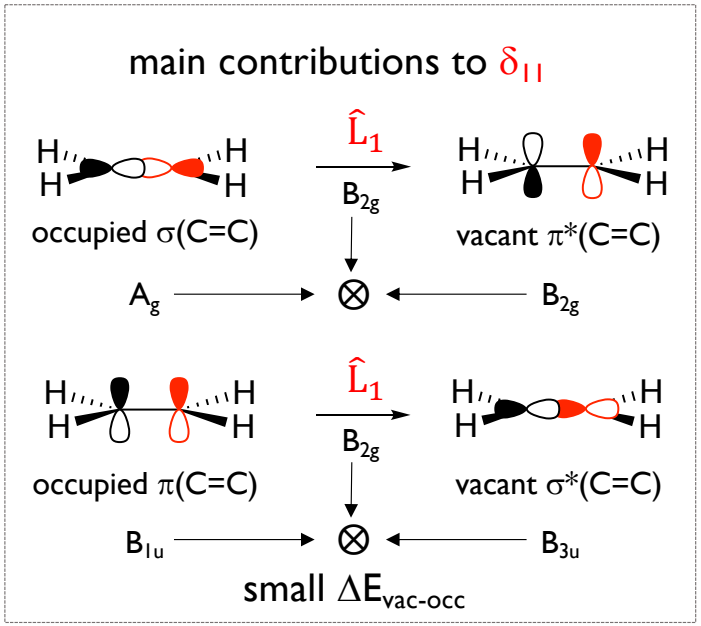

D2h point group

Abelian, 8 irreducible representations

Subgroups: C_s, C_i, C_2, C_{2v}, C_{2h}

Character table

	E	C_2 (z)	C_2 (y)	C_2 (x)	i	σ (xy)	σ (xz)	σ (yz)	linear, rotations	quadratic
A_g	1	1	1	1	1	1	1	1		x^2, y^2, z^2
B_{1g}	1	1	-1	-1	1	1	-1	-1	R_z	xy
B_{2g}	1	-1	1	-1	1	-1	1	-1	R_y	xz
B_{3g}	1	-1	-1	1	1	-1	-1	1	R_x	yz
A_u	1	1	1	1	-1	-1	-1	-1		
B_{1u}	1	1	-1	-1	-1	-1	1	1	z	
B_{2u}	1	-1	1	-1	-1	1	-1	1	y	
B_{3u}	1	-1	-1	1	-1	1	1	-1	x	

Product table

	A_g	B_{1g}	B_{2g}	B_{3g}	A_u	B_{1u}	B_{2u}	B_{3u}
A_g	A_g	B_{1g}	B_{2g}	B_{3g}	A_u	B_{1u}	B_{2u}	B_{3u}
B_{1g}	B_{1g}	A_g	B_{3g}	B_{2g}	B_{1u}	A_u	B_{3u}	B_{2u}
B_{2g}	B_{2g}	B_{3g}	A_g	B_{1g}	B_{2u}	B_{3u}	A_u	B_{1u}
B_{3g}	B_{3g}	B_{2g}	B_{1g}	A_g	B_{3u}	B_{2u}	B_{1u}	A_u
A_u	A_u	B_{1u}	B_{2u}	B_{3u}	A_g	B_{1g}	B_{2g}	B_{3g}
B_{1u}	B_{1u}	A_u	B_{3u}	B_{2u}	B_{1g}	A_g	B_{3g}	B_{2g}
B_{2u}	B_{2u}	B_{3u}	A_u	B_{1u}	B_{2g}	B_{3g}	A_g	B_{1g}
B_{3u}	B_{3u}	B_{2u}	B_{1u}	A_u	B_{3g}	B_{2g}	B_{1g}	A_g

$\langle \pi^*_{C-C} | \hat{L}_1 | \sigma_{C-C} \rangle =$

$\langle \boldsymbol{A_g} | \boldsymbol{B_{2g}} | \boldsymbol{B_{2g}} \rangle = 1$

small $\Delta E_{vac\text{-}occ}$

Larger contribution to Deshielding

$\langle \sigma^*_{C-C} | \hat{L}_1 | \pi_{C-C} \rangle =$

$\langle \boldsymbol{B_{1u}} | \boldsymbol{B_{2g}} | \boldsymbol{B_{3u}} \rangle = 1$

NMR beyond Numbers

Understanding Electronic Structure and Reactivity from NMR

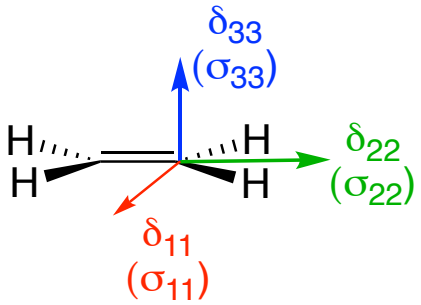

δ_{iso} = 126 ppm

δ_{11} = 234 ppm
δ_{22} = 120 ppm
δ_{33} = 24 ppm

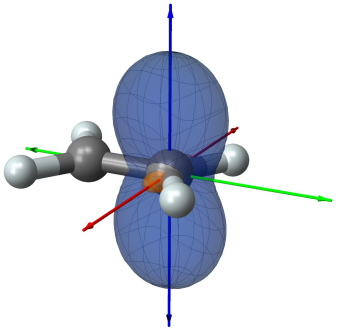

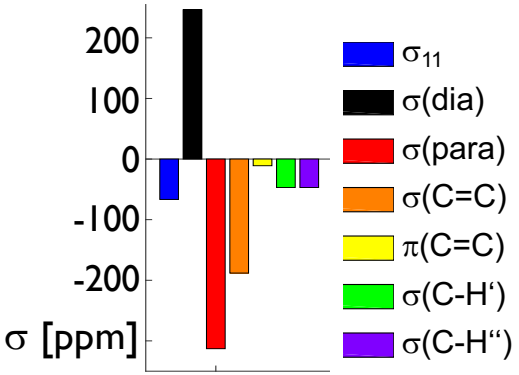

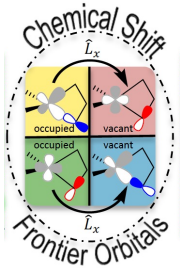

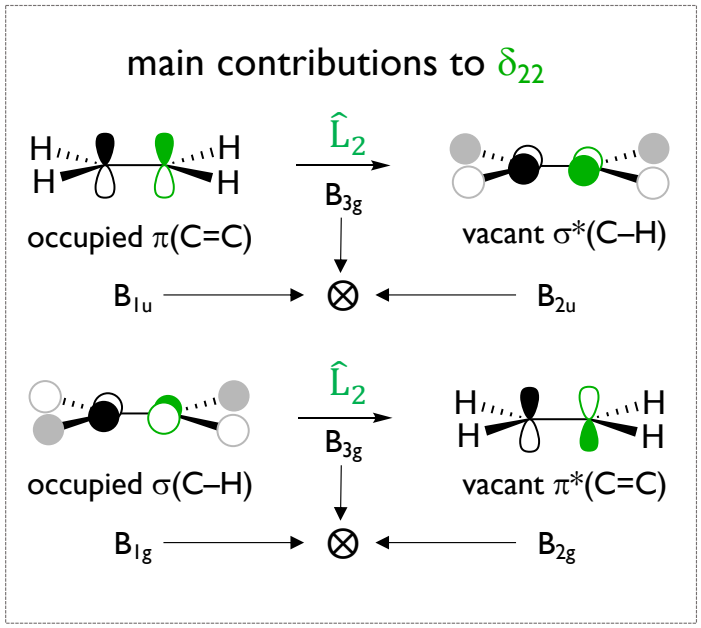

D2h point group

Abelian, 8 irreducible representations

Subgroups: C_s, C_1, C_2, C_{2v}, C_{2h}

Character table

	E	C_2 (z)	C_2 (y)	C_2 (x)	i	σ (xy)	σ (xz)	σ (yz)	linear, rotations	quadratic
A_g	1	1	1	1	1	1	1	1		x^2, y^2, z^2
B_{1g}	1	1	-1	-1	1	1	-1	-1	R_z	xy
B_{2g}	1	-1	1	-1	1	-1	1	-1	R_y	xz
B_{3g}	1	-1	-1	1	1	-1	-1	1	R_x	yz
A_u	1	1	1	1	-1	-1	-1	-1		
B_{1u}	1	1	-1	-1	-1	-1	1	1	z	
B_{2u}	1	-1	1	-1	-1	1	-1	1	y	
B_{3u}	1	-1	-1	1	-1	1	1	-1	x	

Product table

	A_g	B_{1g}	B_{2g}	B_{3g}	A_u	B_{1u}	B_{2u}	B_{3u}
A_g	A_g	B_{1g}	B_{2g}	B_{3g}	A_u	B_{1u}	B_{2u}	B_{3u}
B_{1g}	B_{1g}	A_g	B_{3g}	B_{2g}	B_{1u}	A_u	B_{3u}	B_{2u}
B_{2g}	B_{2g}	B_{3g}	A_g	B_{1g}	B_{2u}	B_{3u}	A_u	B_{1u}
B_{3g}	B_{3g}	B_{2g}	B_{1g}	A_g	B_{3u}	B_{2u}	B_{1u}	A_u
A_u	A_u	B_{1u}	B_{2u}	B_{3u}	A_g	B_{1g}	B_{2g}	B_{3g}
B_{1u}	B_{1u}	A_u	B_{3u}	B_{2u}	B_{1g}	A_g	B_{3g}	B_{2g}
B_{2u}	B_{2u}	B_{3u}	A_u	B_{1u}	B_{2g}	B_{3g}	A_g	B_{1g}
B_{3u}	B_{3u}	B_{2u}	B_{1u}	A_u	B_{3g}	B_{2g}	B_{1g}	A_g

$$\langle \sigma^*_{C-H} | \hat{L}_2 | \pi_{C-C} \rangle =$$

$$\langle \boldsymbol{B_{1u}} | \boldsymbol{B_{3g}} | \boldsymbol{B_{2u}} \rangle = 1$$

$$\langle \pi^*_{C-C} | \hat{L}_2 | \sigma_{C-H} \rangle =$$

$$\langle \boldsymbol{B_{1g}} | \boldsymbol{B_{3g}} | \boldsymbol{B_{2g}} \rangle = 1$$

Larger $\Delta E_{vac\text{-}occ}$

Smaller contribution to Deshielding

NMR beyond Numbers

Understanding Electronic Structure and Reactivity from NMR

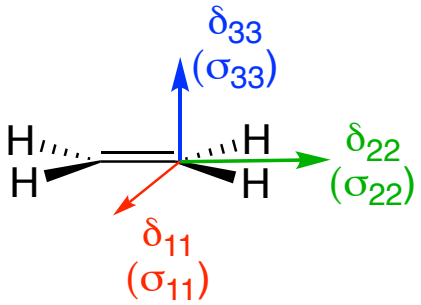

δ_{iso} = 126 ppm

δ_{11} = 234 ppm
δ_{22} = 120 ppm
δ_{33} = 24 ppm

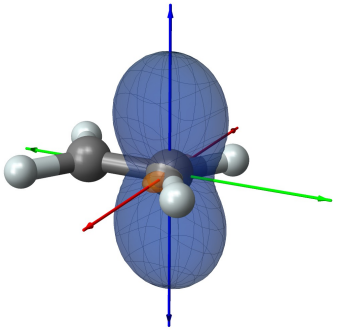

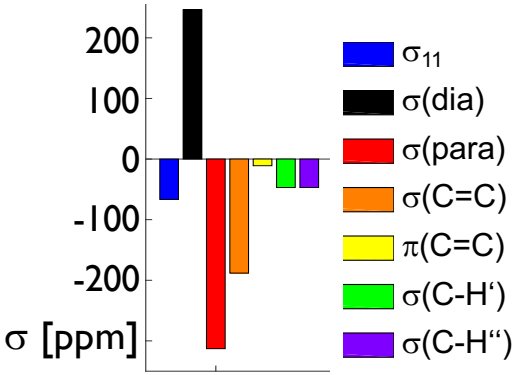

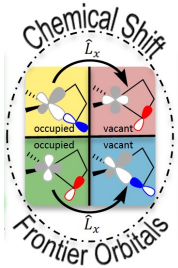

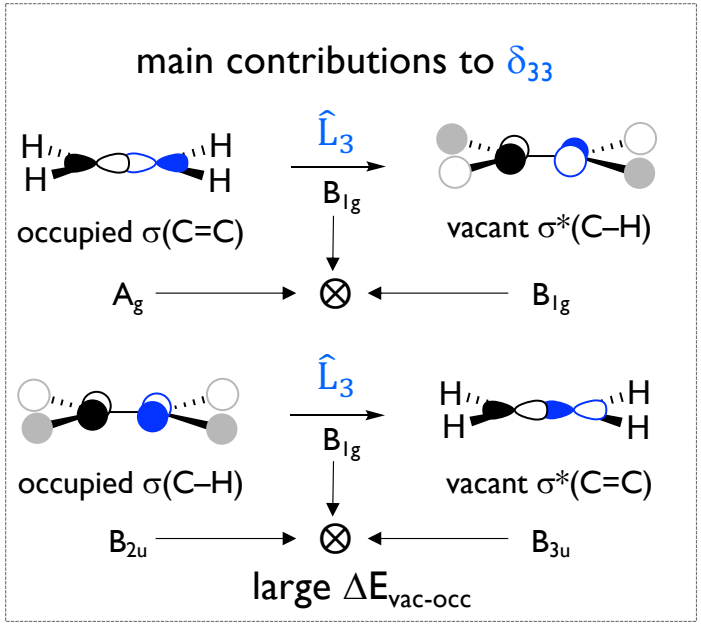

D2h point group

Abelian, 8 irreducible representations

Subgroups: C_s, C_1, C_2, C_{2v}, C_{2h}

Character table

	E	C_2 (z)	C_2 (y)	C_2 (x)	i	σ (xy)	σ (xz)	σ (yz)	linear, rotations	quadratic
A_g	1	1	1	1	1	1	1	1		x^2, y^2, z^2
B_{1g}	1	1	-1	-1	1	1	-1	-1	R_z	xy
B_{2g}	1	-1	1	-1	1	-1	1	-1	R_y	xz
B_{3g}	1	-1	-1	1	1	-1	-1	1	R_x	yz
A_u	1	1	1	1	-1	-1	-1	-1		
B_{1u}	1	1	-1	-1	-1	-1	1	1	z	
B_{2u}	1	-1	1	-1	-1	1	-1	1	y	
B_{3u}	1	-1	-1	1	-1	1	1	-1	x	

Product table

	A_g	B_{1g}	B_{2g}	B_{3g}	A_u	B_{1u}	B_{2u}	B_{3u}
A_g	A_g	B_{1g}	B_{2g}	B_{3g}	A_u	B_{1u}	B_{2u}	B_{3u}
B_{1g}	B_{1g}	A_g	B_{3g}	B_{2g}	B_{1u}	A_u	B_{3u}	B_{2u}
B_{2g}	B_{2g}	B_{3g}	A_g	B_{1g}	B_{2u}	B_{3u}	A_u	B_{1u}
B_{3g}	B_{3g}	B_{2g}	B_{1g}	A_g	B_{3u}	B_{2u}	B_{1u}	A_u
A_u	A_u	B_{1u}	B_{2u}	B_{3u}	A_g	B_{1g}	B_{2g}	B_{3g}
B_{1u}	B_{1u}	A_u	B_{3u}	B_{2u}	B_{1g}	A_g	B_{3g}	B_{2g}
B_{2u}	B_{2u}	B_{3u}	A_u	B_{1u}	B_{2g}	B_{3g}	A_g	B_{1g}
B_{3u}	B_{3u}	B_{2u}	B_{1u}	A_u	B_{3g}	B_{2g}	B_{1g}	A_g

$$\langle \sigma^*_{C-H} | \hat{L}_3 | \sigma_{C-C} \rangle =$$

$$\langle \boldsymbol{A_g} | \boldsymbol{B_{1g}} | \boldsymbol{B_{1g}} \rangle = 1$$

Large $\Delta E_{vac\text{-}occ}$

$$\langle \sigma^*_{C-C} | \hat{L}_3 | \sigma_{C-H} \rangle =$$

$$\langle \boldsymbol{B_{2u}} | \boldsymbol{B_{1g}} | \boldsymbol{B_{3u}} \rangle = 1$$

NMR beyond Numbers

Understanding Electronic Structure and Reactivity from NMR

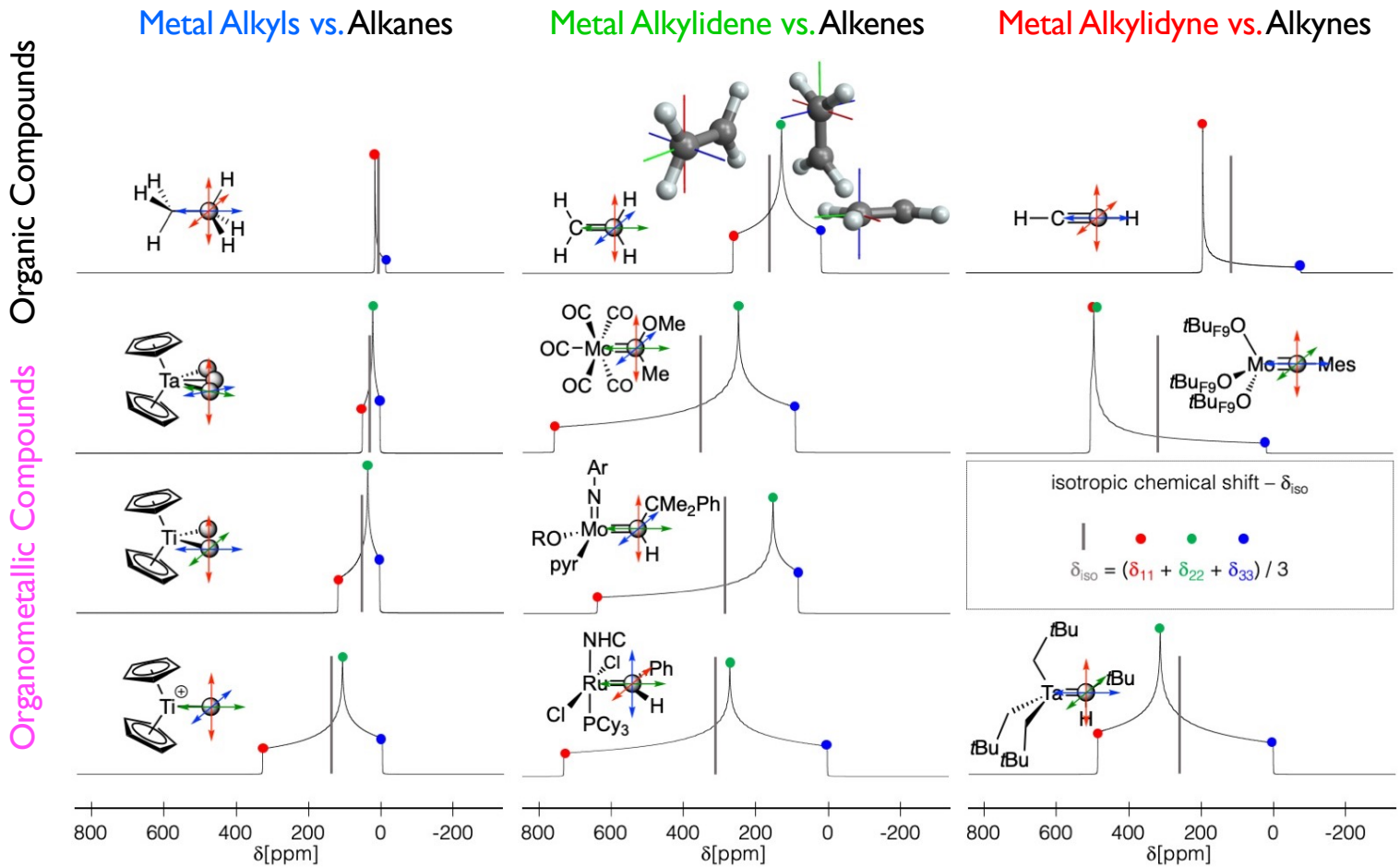

Can we Understand Changes in Electronic Structures from Chemical Shift ?

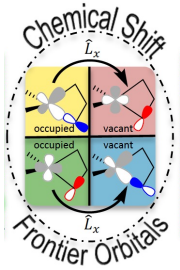

NMR beyond Numbers

Understanding Electronic Structure and Reactivity from NMR

Step I: Experimental (solid-state NMR)
Measurement of principal components δ_{ii}

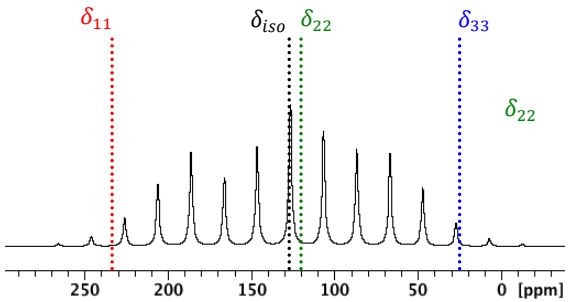

$$\delta_{iso} = \frac{1}{3}(\delta_{11} + \delta_{22} + \delta_{33})$$

Step II: DFT calculation of shielding tensors:
Principal components and orientation

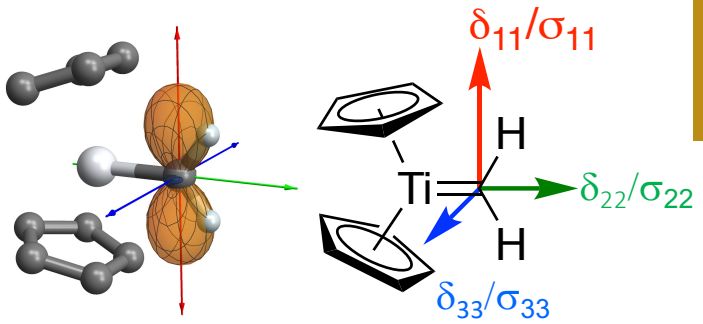

See Len Mueller's Presentation

Step III: Natural Chemical Shift (NCS) analysis:
Determination of orbital contributions to shielding

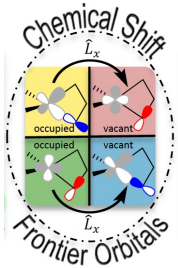

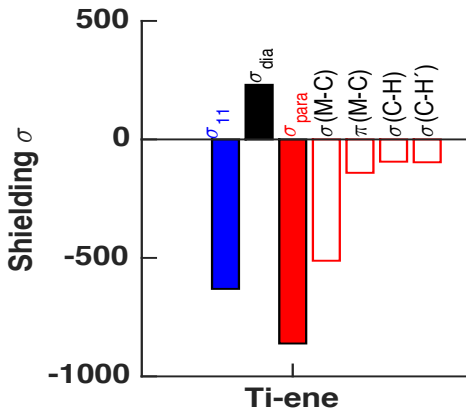

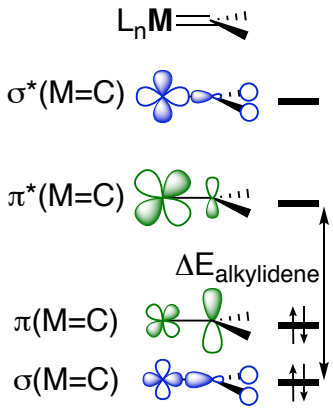

Key orbitals
for
NMR Chemical Shift

Molecular Orbitals involved in Chemical Shielding (σ_{11}) in Metal Carbenes

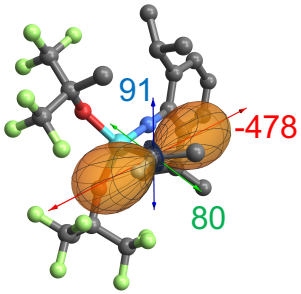

Mo Schrock alkylidene
(Nucleophilic/Metathesis Cat)

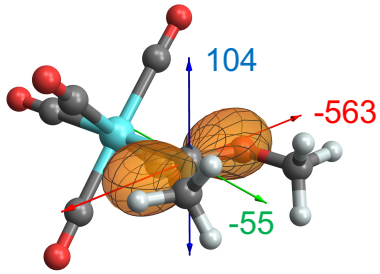

Mo Fischer carbene
Electrophilic/cyclopropanation

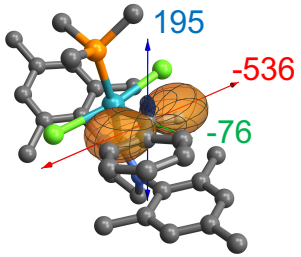

Ru Grubbs-system

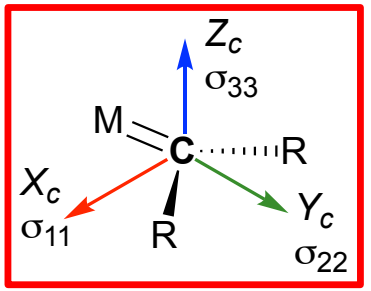

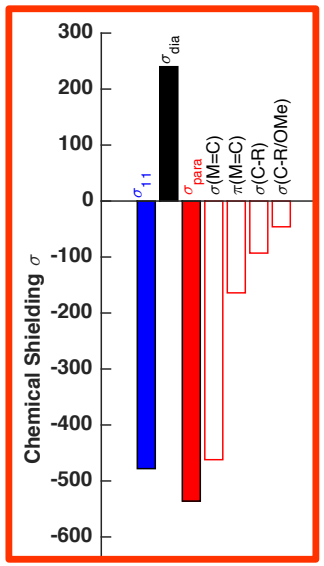

σ_{11}

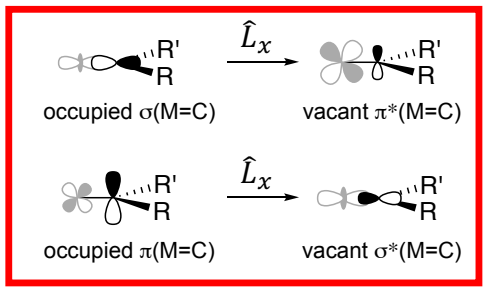

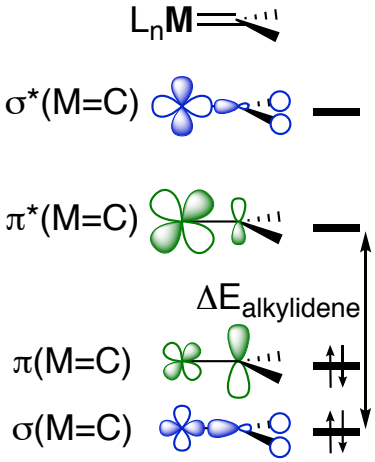

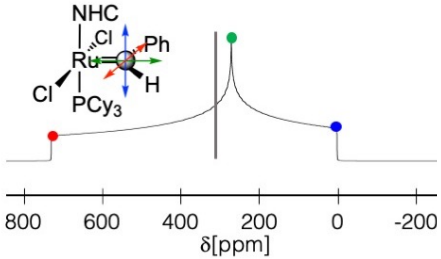

- OR substituent raises π*(M=C)
- CO, a π-acceptor ligand lowers π*(M=C), hence the electrophilicity of Fischer carbenes
- ΔE increass as follows 3d > 4d > 5d metals, explaining the observed δ_{iso}

Halbert *et al.* J. Am. Chem. Soc. **2016**, *138*, 2261.
Yamamoto, Gordon *et al.* Angew. Chem. Int. Ed. **2017**, *56*, 10127.

NMR beyond Numbers

Understanding Electronic Structure and Reactivity from NMR

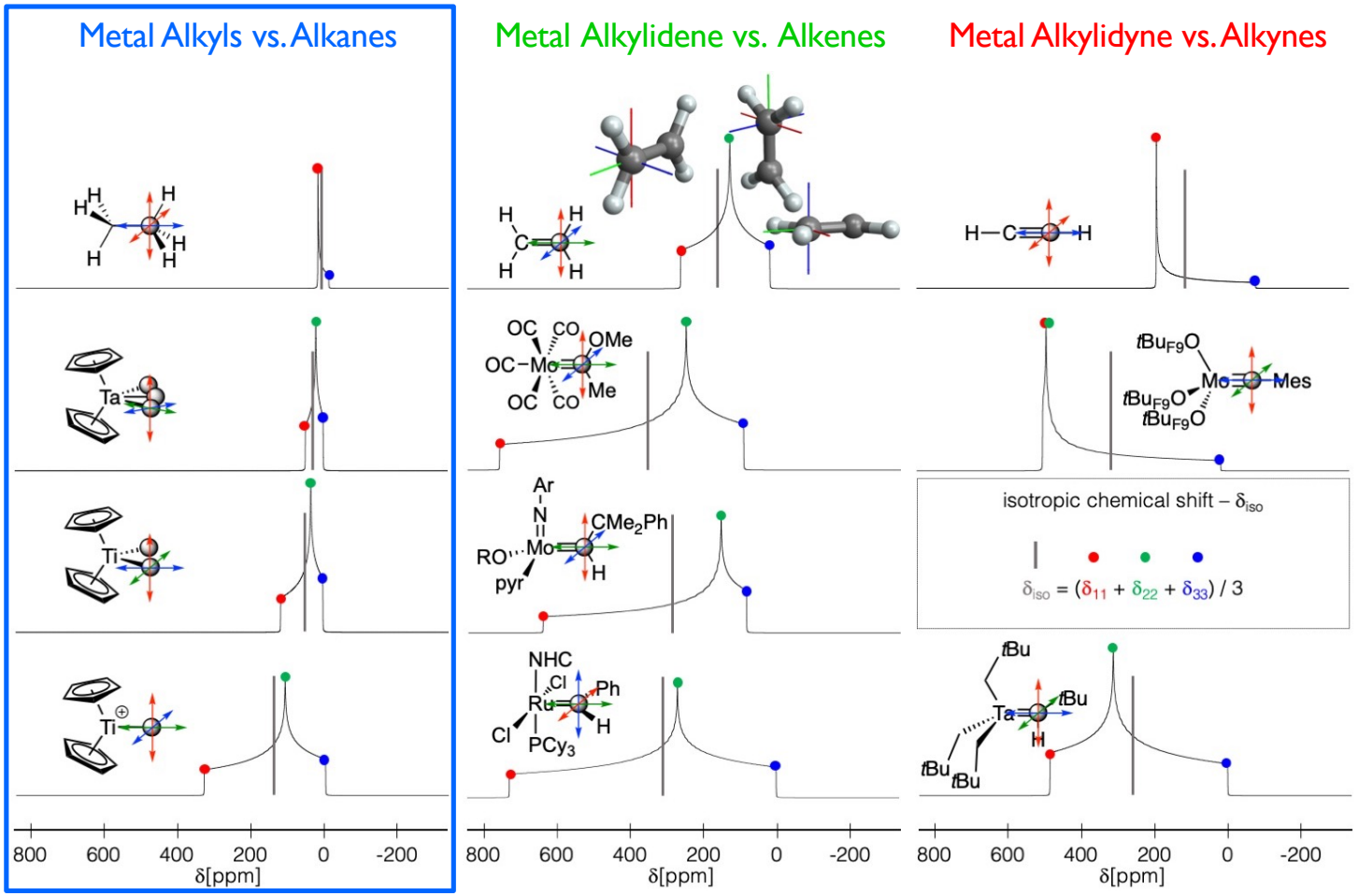

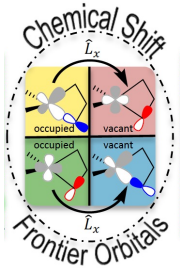

Can we Understand Changes in Electronic Structures from Chemical Shift ?

NMR beyond Numbers

Understanding Electronic Structure and Reactivity from NMR

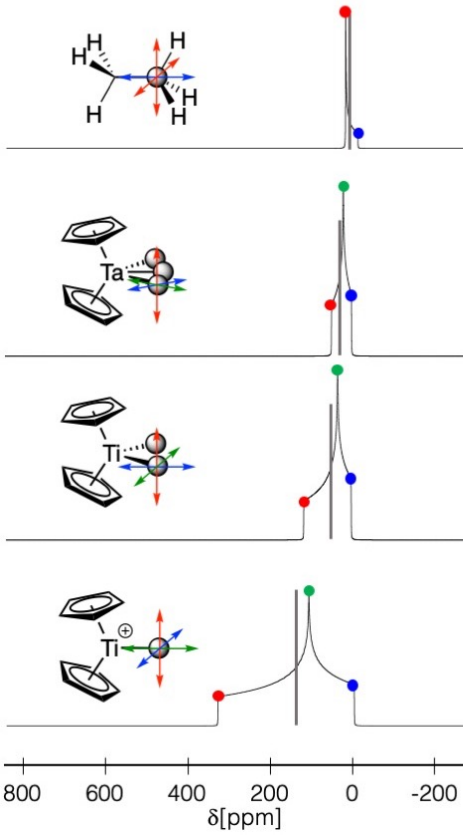

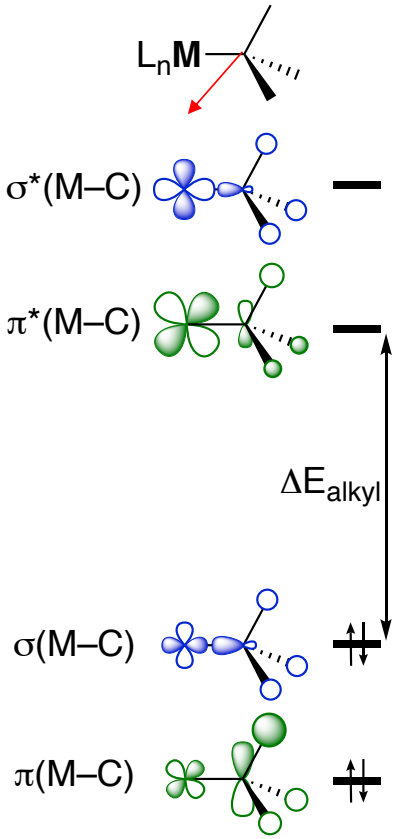

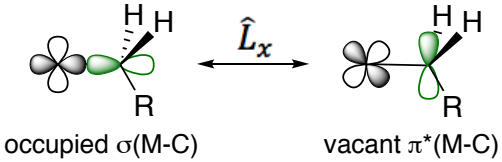

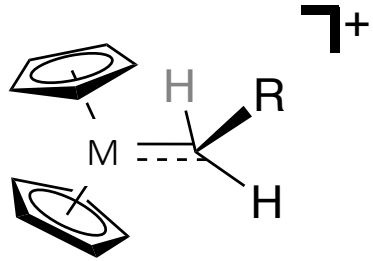

Alkylidenic Character:
a Key to Reactivity
Insertion = [2+2]-cycloaddition!

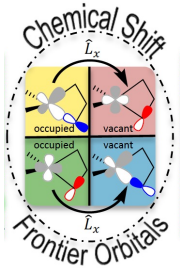

Gordon, Yamamoto, Shirase et al. PNAS **2018**, *115*, E5867-E5876

Measuring/Evaluating Acidity and Basicity in solids

a)

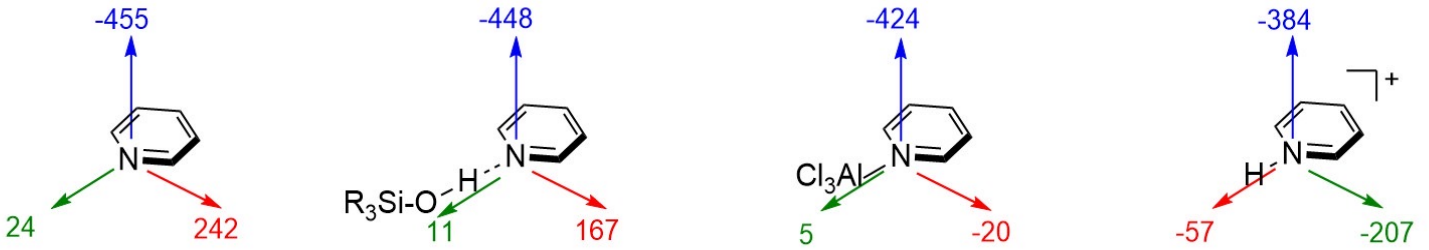

b)

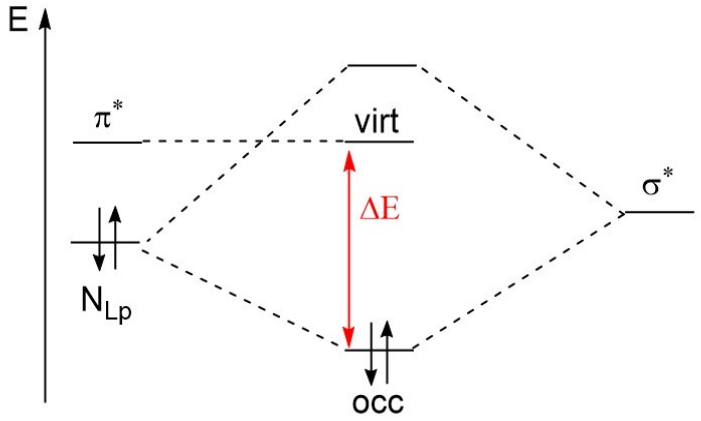

strong adsorption = high ΔE = small deshielding

c)

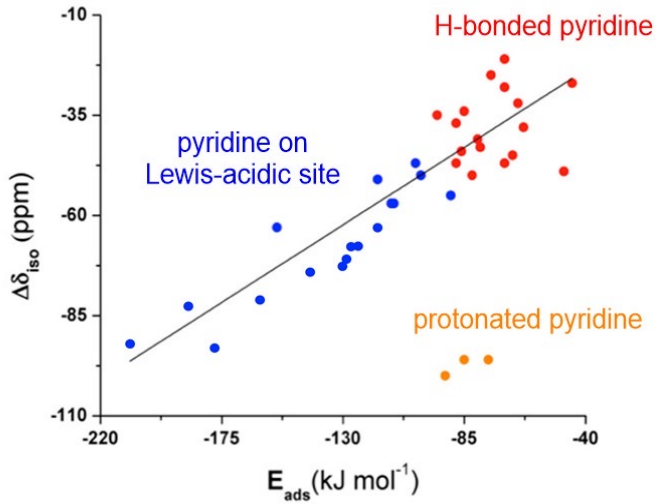

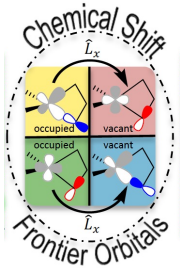

I. B. Moroz, K. Larmier, W.-C. Liao, C. Copéret, *J. Phys. Chem. C.* 2018, *122*, 10871–10882

NMR beyond Numbers

Understanding Electronic Structure and Reactivity from NMR – Concept

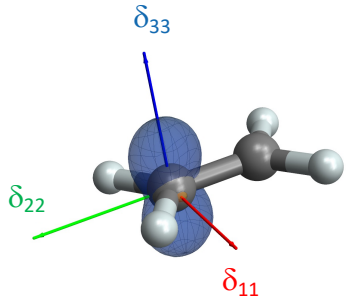

Solid-State NMR Spectroscopy – Chemical Shift Anisotropy

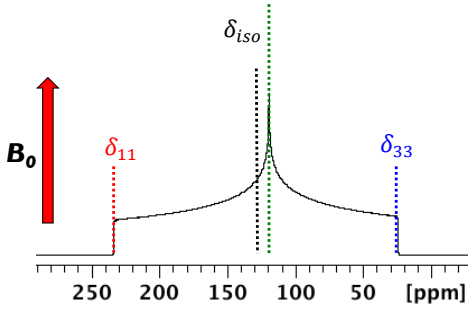

$$\sigma = \sigma_{dia} + \sigma_{para+SO}$$

$$\sigma_{ii,para} \Leftrightarrow \frac{\langle \Psi_{vac}|\hat{L}_i|\Psi_{occ}\rangle\langle \Psi_{vac}|\hat{L}_i/r^3|\Psi_{occ}\rangle}{\Delta E_{vac-occ}}$$

Chemical Shift (Tensors),
a Reactivity Descriptor

Frontier
Molecular Orbitals

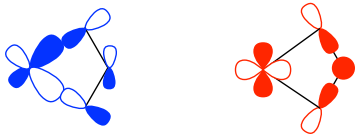

Reactivity

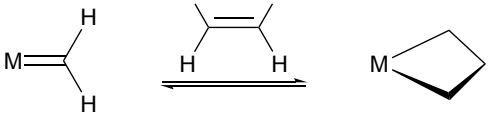

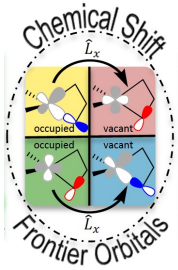

C. P. Gordon, L. Lätsch, CCH *J. Phys. Chem. Lett.* 2021, 12, 2072.
C.P. Gordon, C. Raynaud, R.A. Andersen, C. Copéret, O. Eisenstein, *Acc. Chem. Res.* 2019, 52, 2278.
C. P. Gordon, R. A. Andersen, CCH *Helvetica Chim Acta* 2019, 102, e1900151 (Tutorial)

NMR beyond Numbers: Solving Structure of Complex Hybrid Organic Inorganic Materials from Metal NMR

Development of Heterogeneous Catalysts and Functional Materials via a Molecular Approach

A case study:
Ziegler-Nata Catalysts

Complex Hybrid Materials prepared in multiple steps
Based on a transition metal chloride
($TiCl_4$), $MgCl_2$, organic modifiers ….

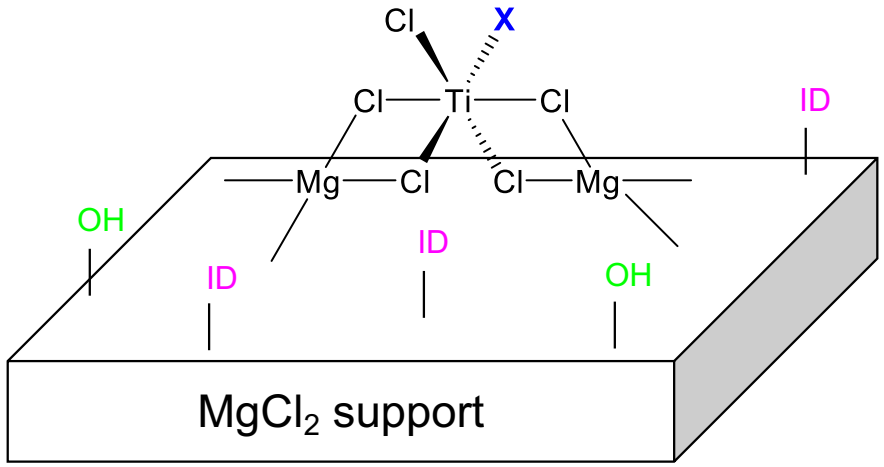

X = Cl, OR, ID

Complex hybrid material!

1. AlR_3/ED/heptane

2. C_2H_4 or C_3H_6

Responsible for the Worldwide production

PE (> 50%) PP (> 95%)

NMR beyond Numbers: Solving Structure of Complex Hybrid Organic Inorganic Materials from Metal NMR

Development of Heterogeneous Catalysts and Functional Materials via a Molecular Approach

A case study: Ziegler-Nata Catalysts

Step 1
Support activation

Step 2
Metal deposition

Step 3
Catalyst activation

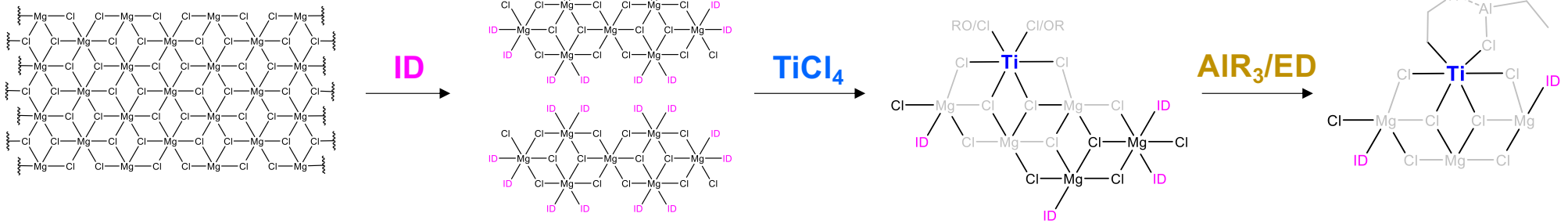

Crystalline α(β)-$MgCl_2$

$MgCl_2$-ID nanoclusters
Decreased Crystallinity

ZN pre-catalysts
Partial or Complete Amorphization

Activated ZNC

ID (internal donor) – ether or ester (for PP) and THF or ethanol (for PE)

ED (external donor) – alkyl alkoxysilane (for PP)

Need for detailed understanding of surface sites at all stages!

NMR beyond Numbers: Solving Structure of Complex Hybrid Organic Inorganic Materials from Metal NMR

Development of Heterogeneous Catalysts and Functional Materials via a Molecular Approach

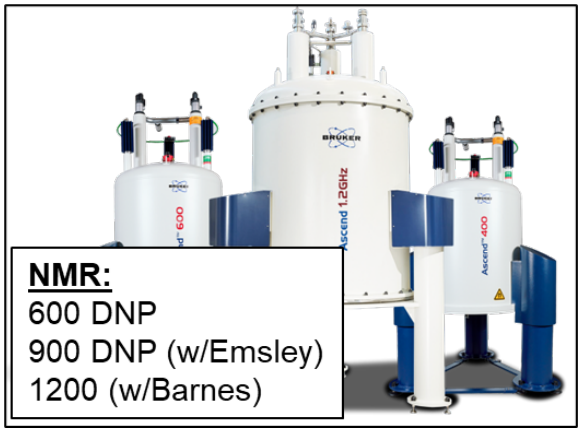

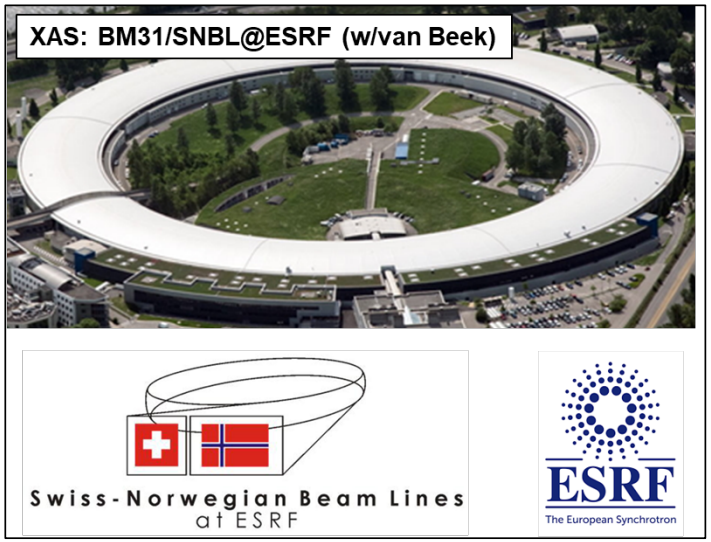

$MgCl_2 \bullet 1.5THF$ $\xrightarrow{TiCl_4}$ 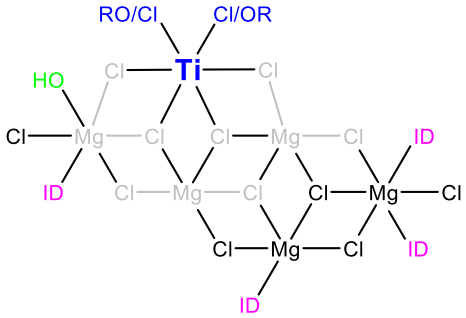 $\xrightarrow[-B(OR)_3]{BCl_3}$ 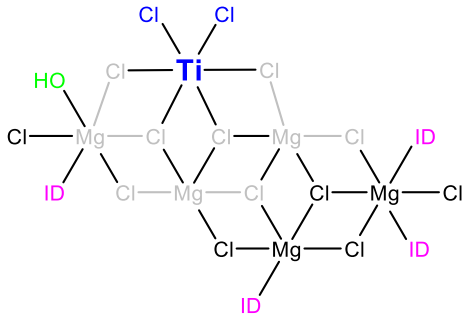 $\xrightarrow{AlR_3/ED}$ 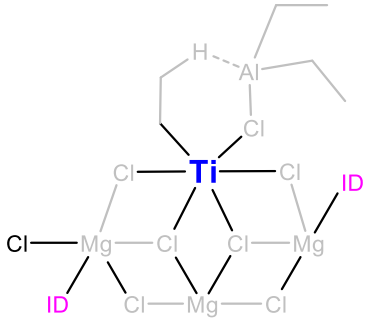

ZN pre-catalysts ***Modified ZN pre-catalysts*** ***Activated ZN catalyst***

Collaboration with Monteil (Since 2010), Barnes, Busico, Emsley, Groppo, Jeschke, Lesage, Pintacuda, Raynaud, Sautet, Taniike…

NMR beyond Numbers

Understanding Electronic Structure and Reactivity from NMR

A case study:
Ziegler-Nata Catalysts

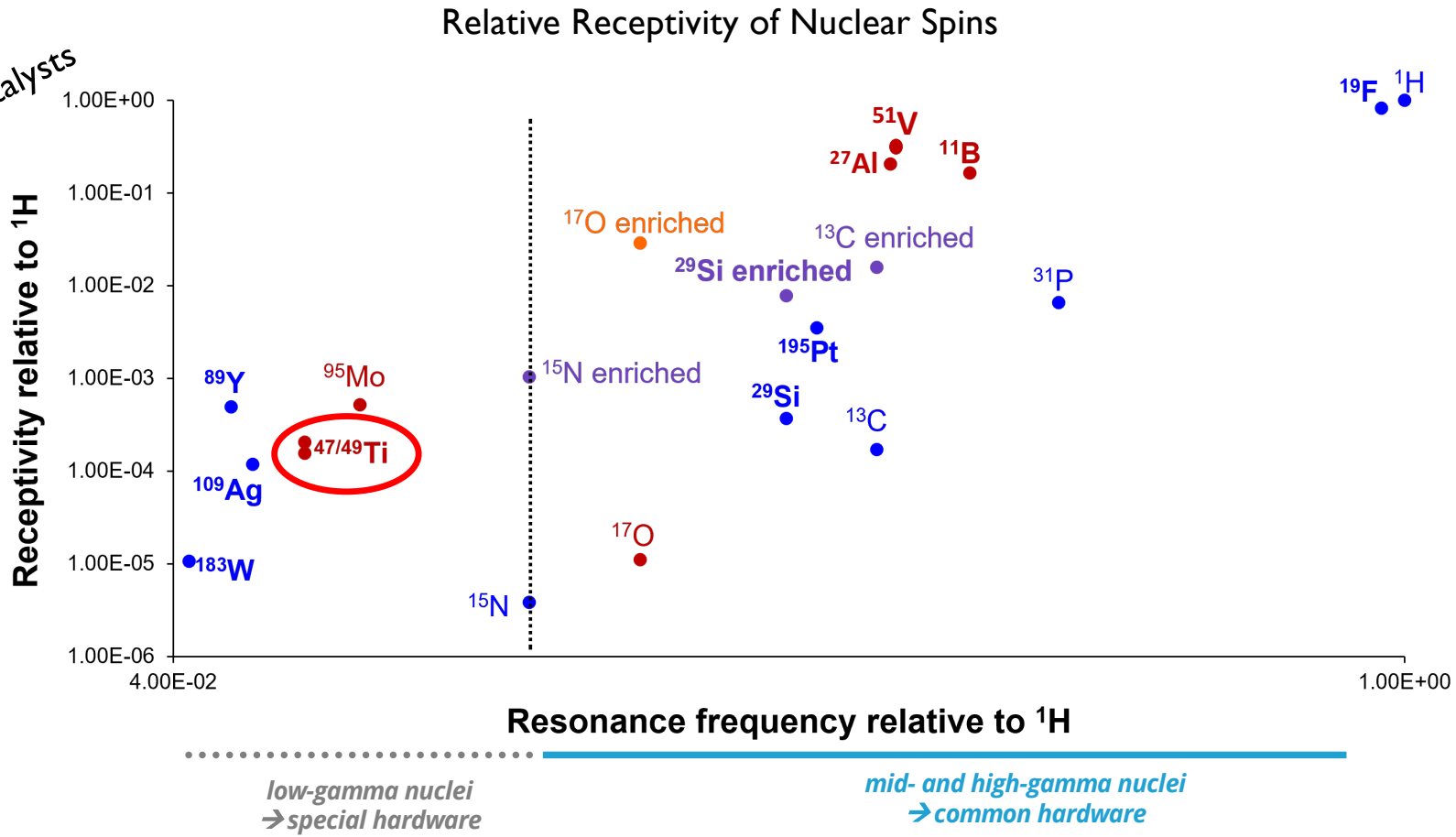

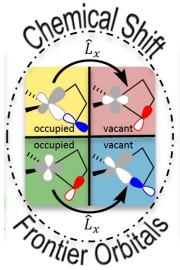

- New advances in solid-state NMR instrumentation (fast-MAS probes, higher fields, DNP) to overcome challenges of sensitivity, accessibility

NMR beyond Numbers

Understanding Electronic Structure and Reactivity from NMR

For molecular compounds (e.g. titanocenes)

Cp_2TiCl_2 $Cp^*_2TiCl_2$

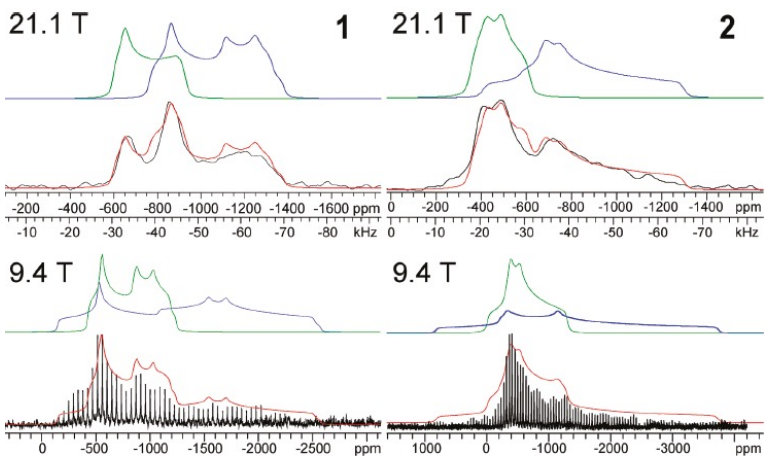

- High information content on electronic structure
- But: Measurement only possible because of rel. high Ti wt% loading and small C_Qs (< 5 MHz)

For bulk oxides (e.g. rutile, anatase, …)

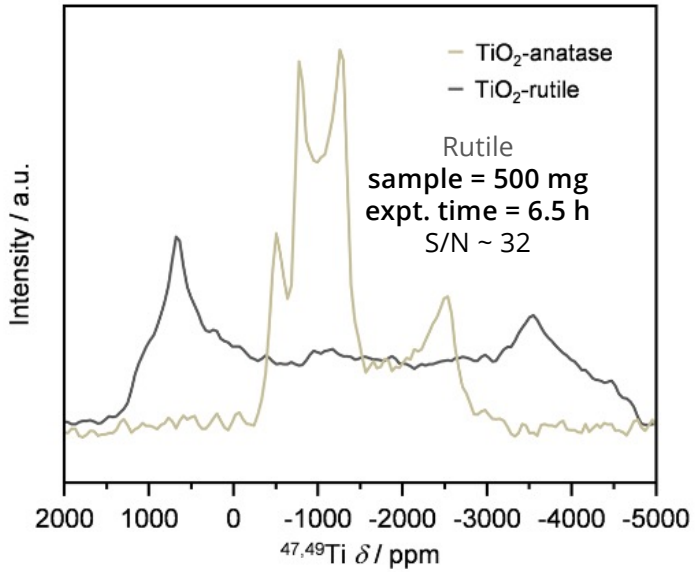

- Broad signals (e.g. rutile C_Q = 14 MHz) require long expt. time despite high Ti wt% loading

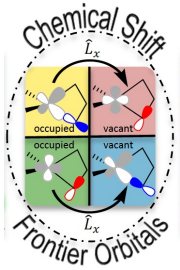

Stephens *et al. Catal. Sci. Tech.* 2020, *10*, 4072–4083
Rossini *et al. J. Phys. Chem. Lett.* 2010, *1*, 2989 – 2998

NMR beyond Numbers

Understanding Electronic Structure and Reactivity from NMR

A case study: Ziegler-Nata Catalysts

	Nat. abund. (%)	Receptivity (relative to ^{13}C)	Spin
^{47}Ti	7.44	0.918	5/2
^{49}Ti	5.41	1.200	7/2

- Chemical shift tensor: δ_{iso}, Ω, κ — Partially averaged by MAS
- efg tensor: C_Q, η_Q — Field dependent
- Euler angles: φ, χ, ψ — Relative orientations of two tensors

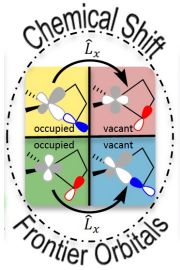

Signals from ^{47}Ti and ^{49}Ti overlap, especially at lower fields

High fields and intermediate MAS rates (> 15 kHz) necessary

Simulated $^{47/49}Ti$ NMR (static)

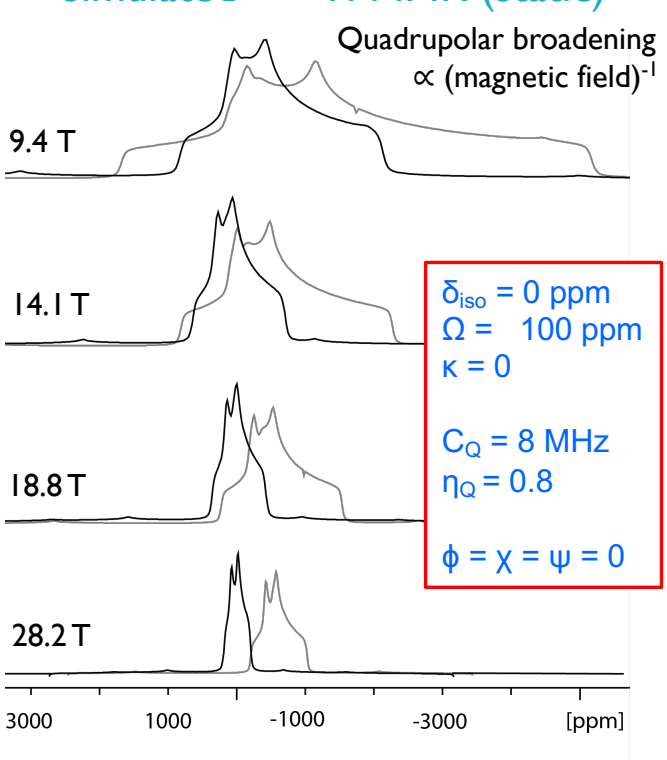

Simulated $^{47/49}Ti$ NMR @ 18.8 T

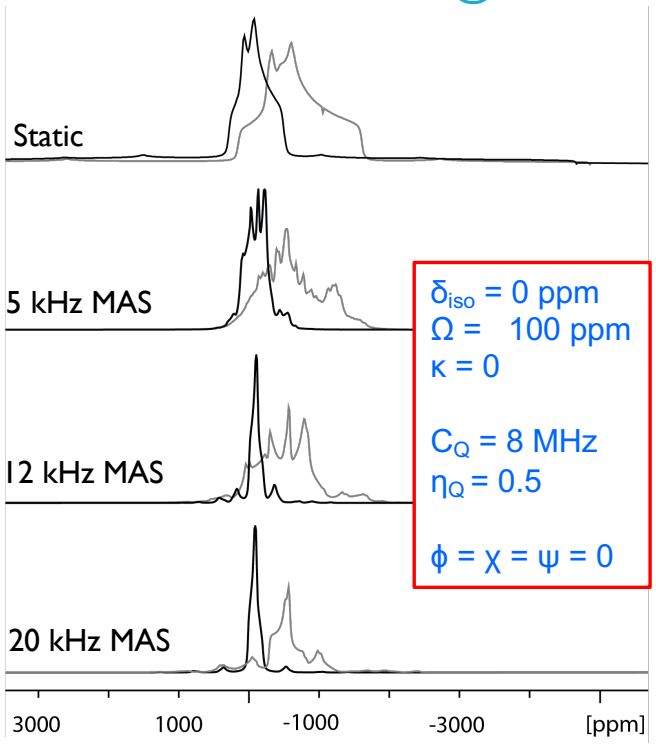

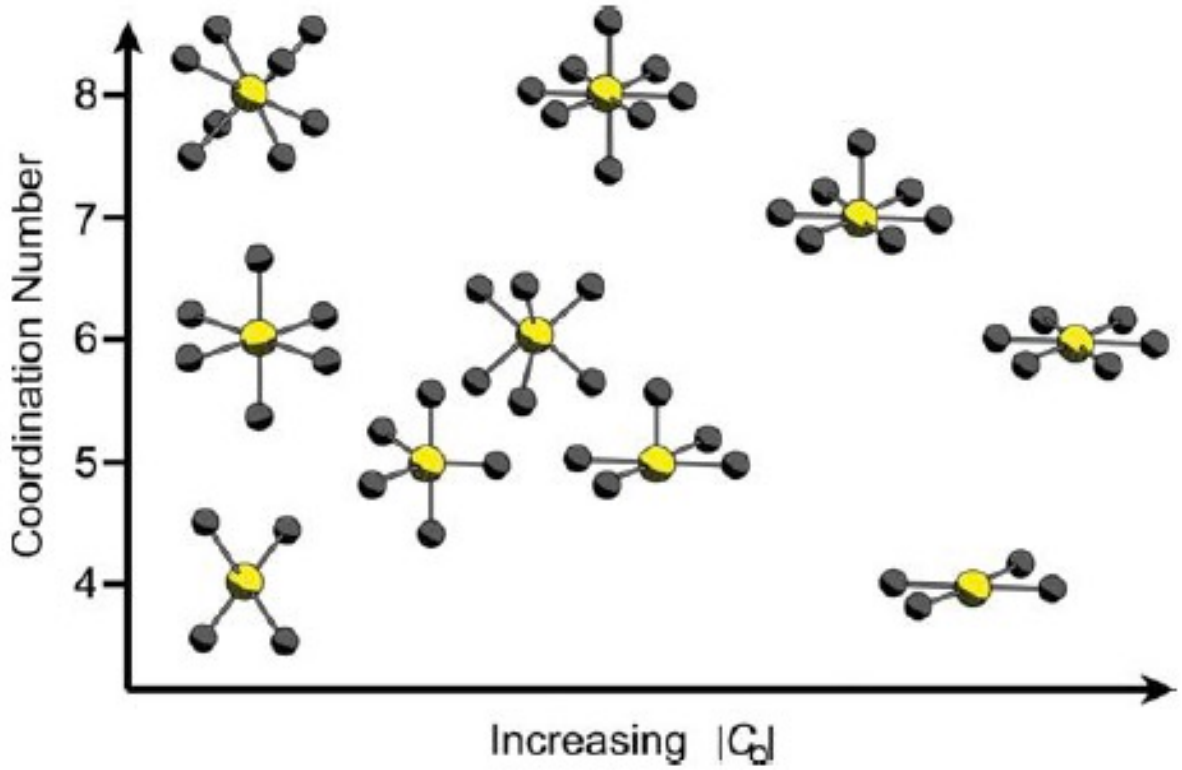

See Phil Grandinetti's Presentation

Analysis of Electric Field Gradient Tensors at Quadrupolar Nuclei in Common Structural Motifs
J. Autschbach, S. Zheng, R. W. Schurko Concepts Magn. Res. A 2010, 36A, 84–126

NMR beyond Numbers

Understanding Electronic Structure and Reactivity from NMR

A case study:
Ziegler-Nata Catalysts

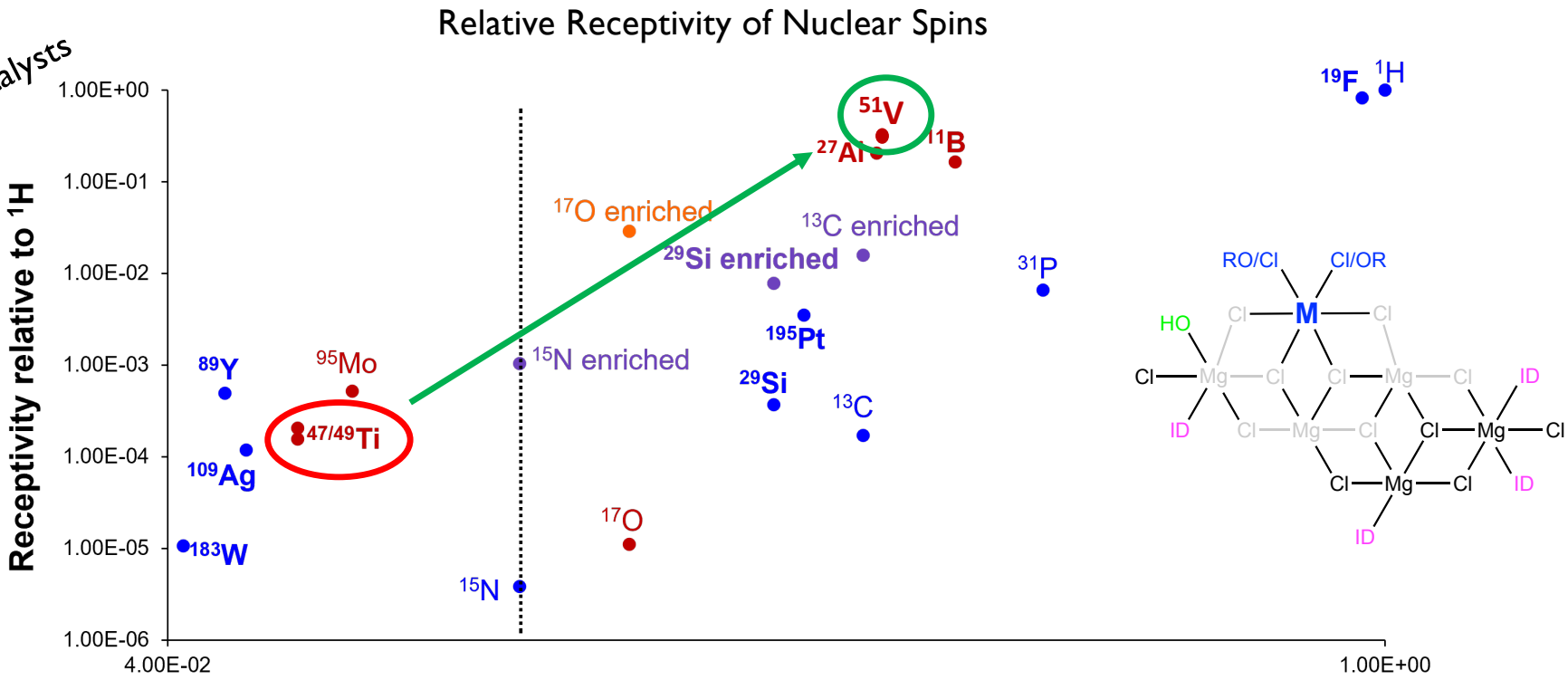

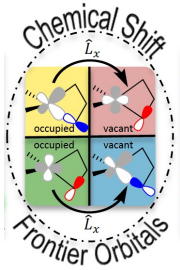

S. Sabisch, Y. Kakiuchi, S. R. Docherty, A. V. Yakimov, CCH
J. Am. Chem. Soc. 2023, *145*, 25595–25603. DOI: 10.1021/jacs.3c06200

Ziegler-Natta Catalysis – Understanding the Structure of Surface Sites by NMR

Nucleus	^{47}Ti	^{49}Ti	^{51}V
Spin	5/2	7/2	7/2
Natural abundance, %	7.44	5.41	**99.75**
Frequency at 21.1 T, MHz	50.745	50.759	**236.761**
Frequency at 28.1 T, MHz	67.660	67.679	**315.681**
Electric quadrupole moment, b	0.30	0.24	**-0.04**
Receptivity relative to ^{13}C	0.918	1.20	**2250**

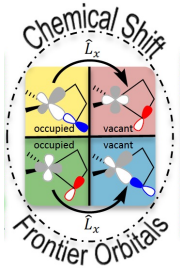

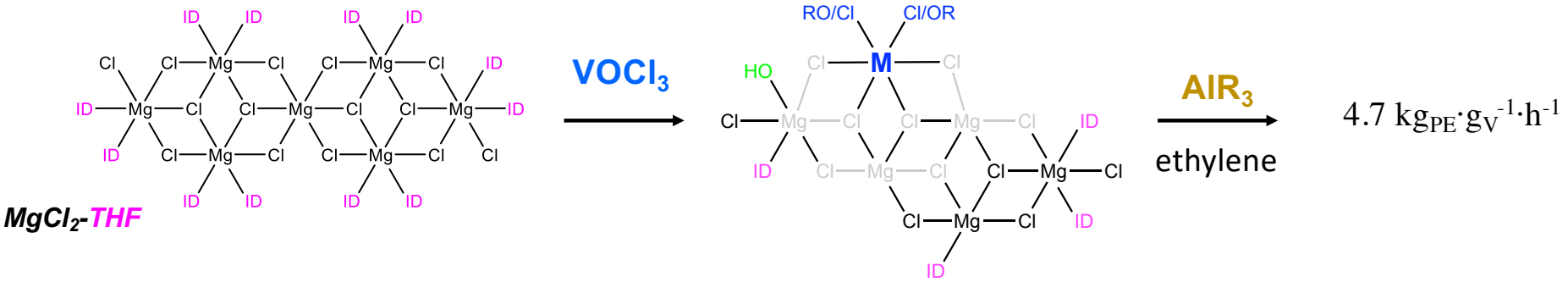

- ^{51}V: Sensitive NMR
- $VOCl_3$ isoelectronic with $TiCl_4$!
- V-based ZNC are known for co-polymerization

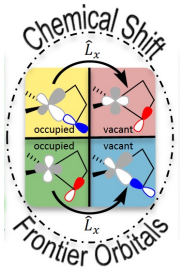

S. Sabisch, Y. Kakiuchi, S. R. Docherty, A. V. Yakimov, CCH
J. Am. Chem. Soc. 2023, *145*, 25595–25603.

NMR beyond Numbers

Understanding Electronic Structure and Reactivity from NMR

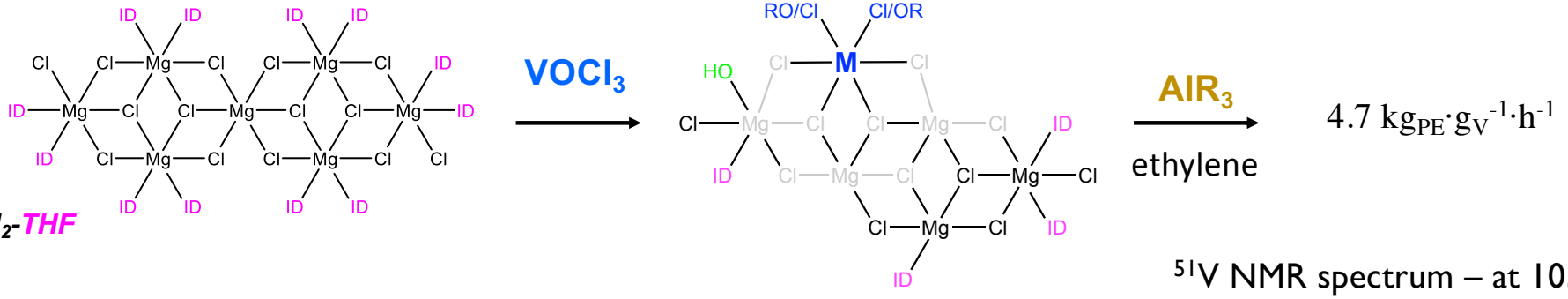

$MgCl_2$-*THF*

- **^{51}V: Sensitive NMR**
- **$VOCl_3$ isoelectronic with $TiCl_4$!**
- **V-based ZNC are known for co-polymerization**

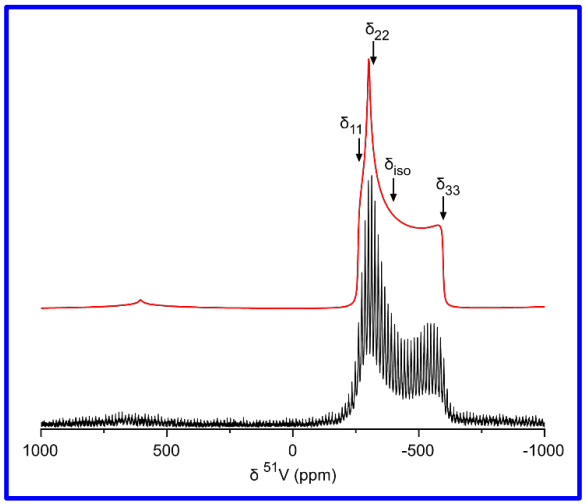

^{51}V NMR spectrum – at 103 K & 14.1 T using WURST-QCPMG pulse sequence

A single NMR signature

dominated by Chemical Shift Anisotropy

indicating A Well-Defined Species for V-based ZN pre-catalysts

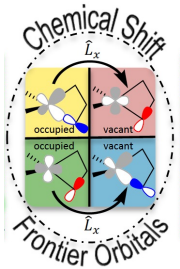

S. Sabisch, Y. Kakiuchi, S. R. Docherty, A. V. Yakimov, CCH
J. Am. Chem. Soc. 2023, *145*, 25595–25603. DOI: 10.1021/jacs.3c06200

NMR beyond Numbers

Understanding Electronic Structure and Reactivity from NMR

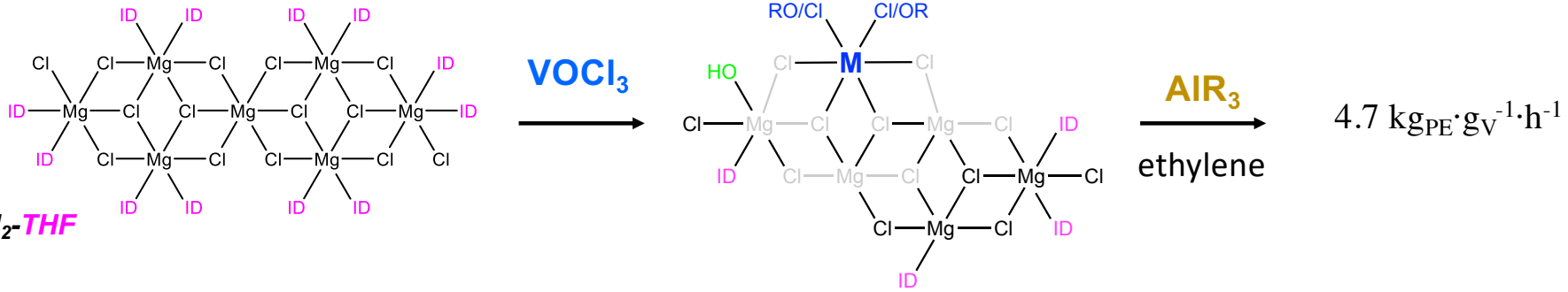

- ^{51}V: Sensitive NMR
- $VOCl_3$ isoelectronic with $TiCl_4$!
- V-based ZNC are known for co-polymerization

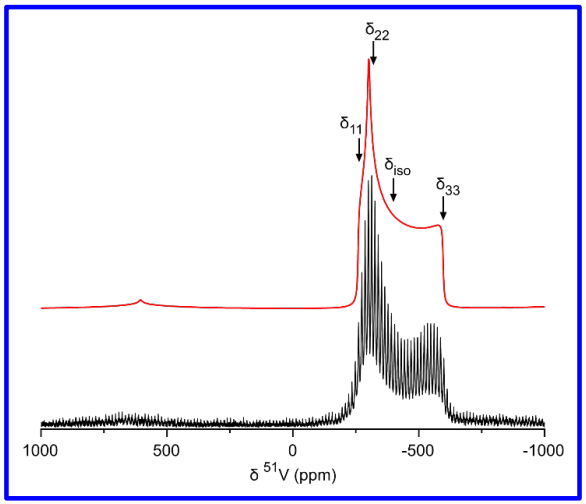

A NMR signature

Nature of Ligands bound to V?

Nature of Geometry and Local Environment?

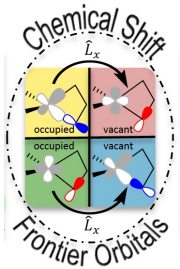

S. Sabisch, Y. Kakiuchi, S. R. Docherty, A. V. Yakimov, CCH
J. Am. Chem. Soc. 2023, *145*, 25595–25603. DOI: 10.1021/jacs.3c06200

NMR beyond Numbers

Understanding Electronic Structure and Reactivity from NMR

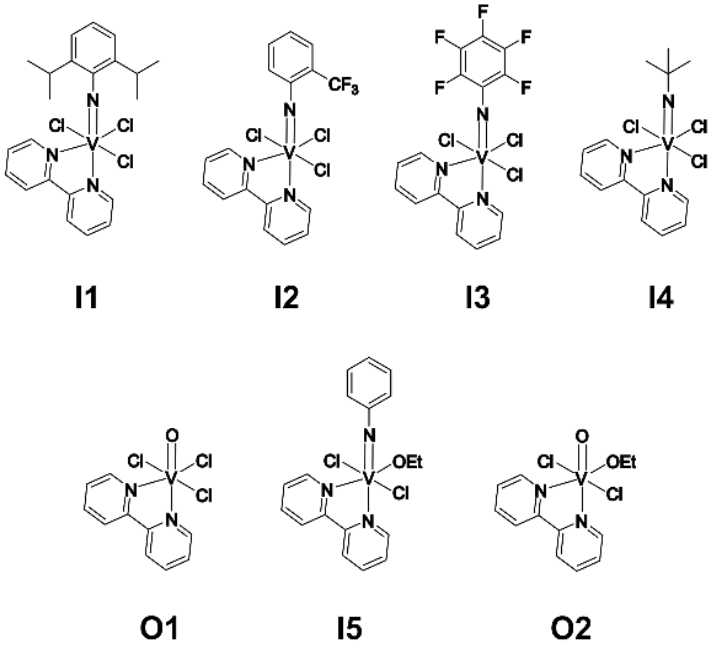

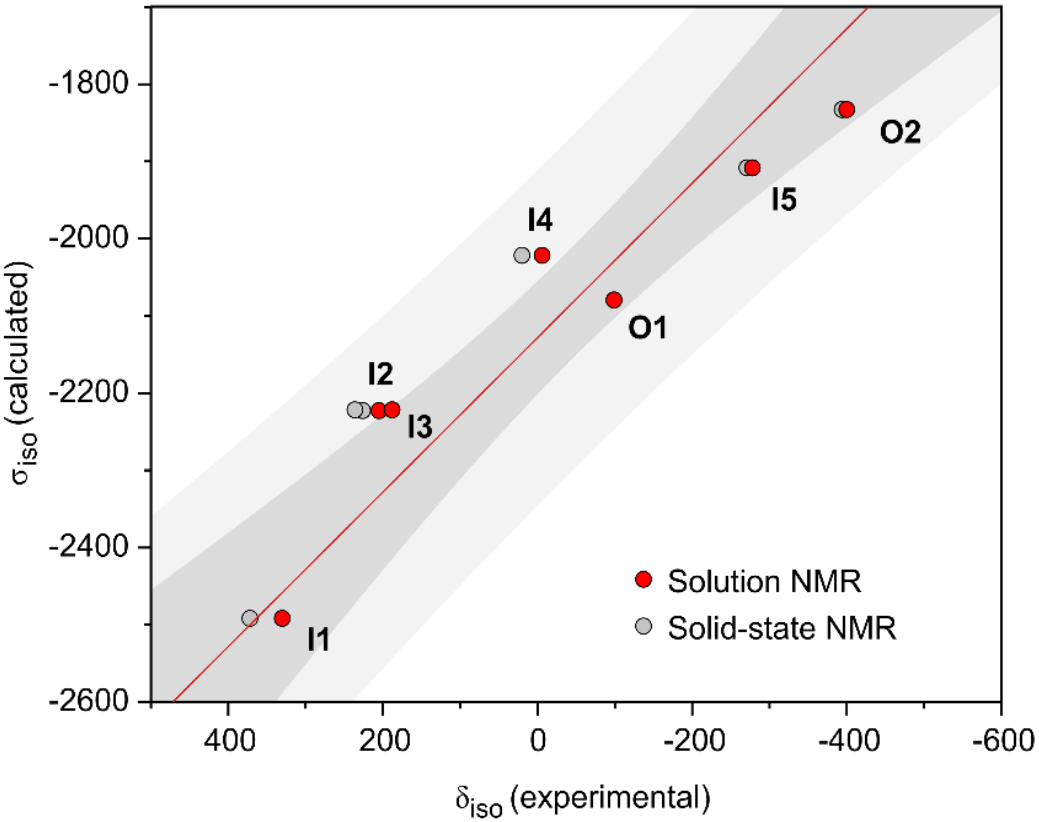

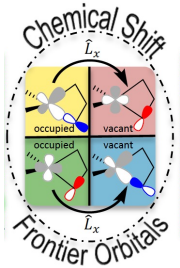

Level of Calculations: B3LYP/Def2TZVP

S. Sabisch, Y. Kakiuchi, S. R. Docherty, A. V. Yakimov, CCH
J. Am. Chem. Soc. 2023, *145*, 25595–25603. DOI: 10.1021/jacs.3c06200

NMR beyond Numbers

Understanding Electronic Structure and Reactivity from NMR

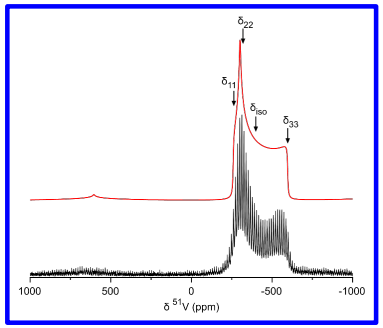

Effect of Geometry: [4], [5] vs. [6] coordinated

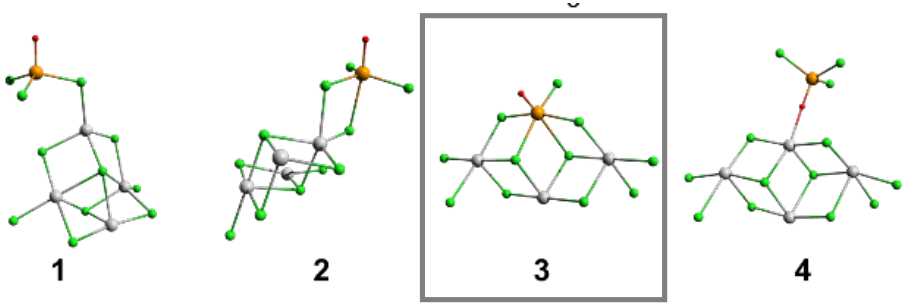

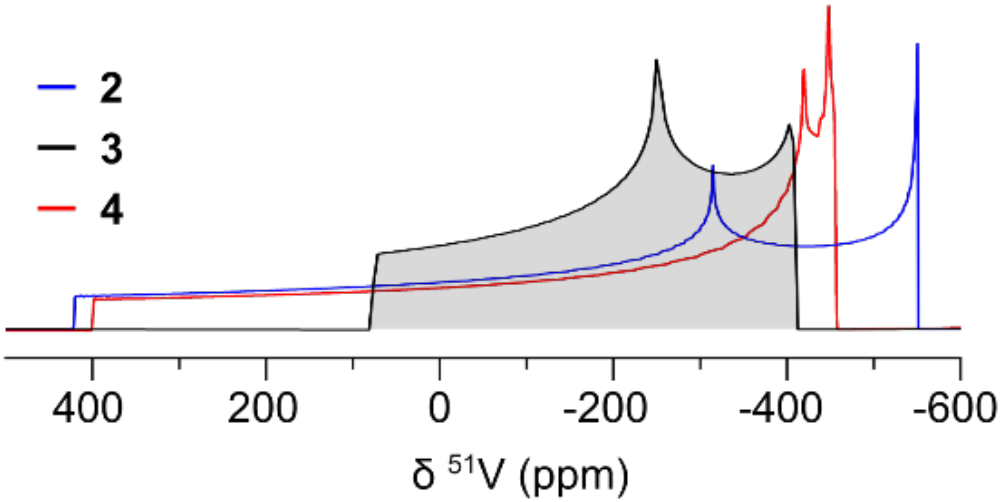

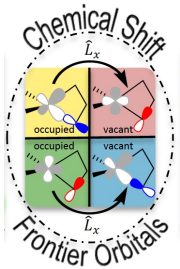

S. Sabisch, Y. Kakiuchi, S. R. Docherty, A. V. Yakimov, CCH
J. Am. Chem. Soc. 2023, *145*, 25595–25603.

NMR beyond Numbers

Understanding Electronic Structure and Reactivity from NMR

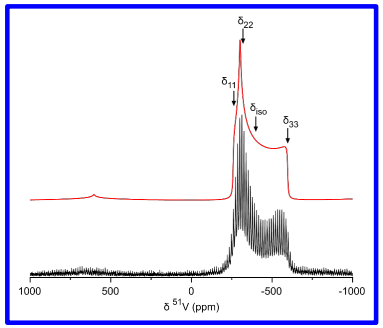

Effect of Anionic Ligands

3a

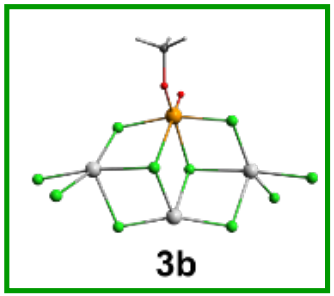

3b

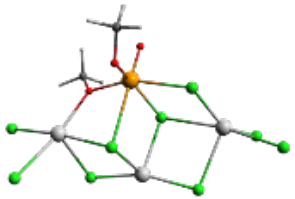

3c

Effect of Geometry

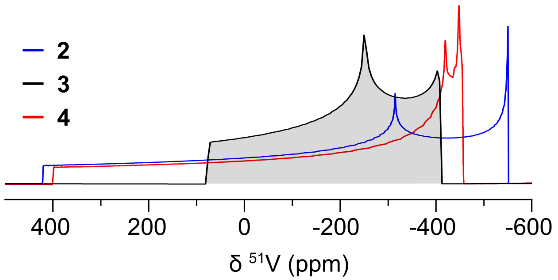

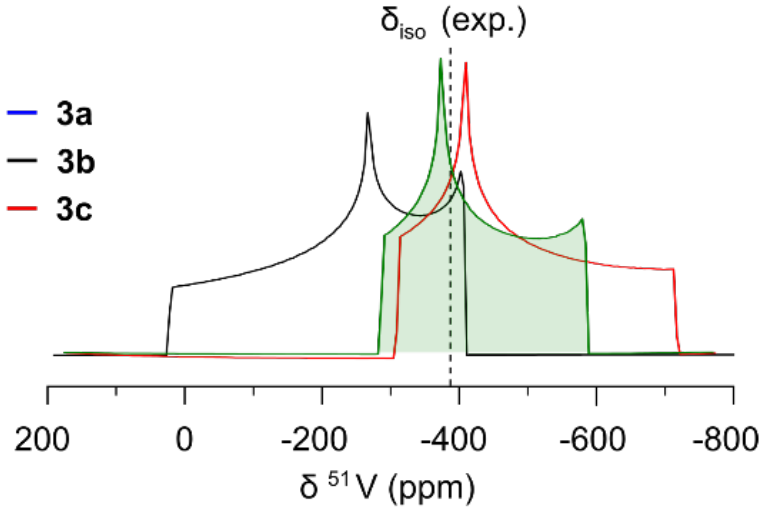

Level of Calculations:
B3LYP/Def2TZVP / Cluster Models

S. Sabisch, Y. Kakiuchi, S. R. Docherty, A. V. Yakimov, CCH
J. Am. Chem. Soc. 2023, *145*, 25595–25603.

NMR beyond Numbers

Understanding Electronic Structure and Reactivity from NMR

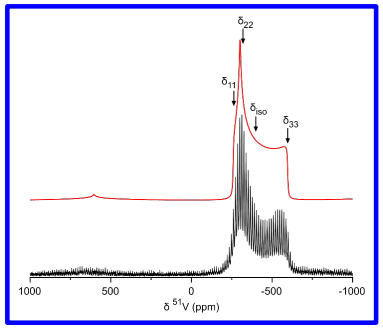

Support Effect – from Crystalline (110) to Amorphous $MgCl_2$

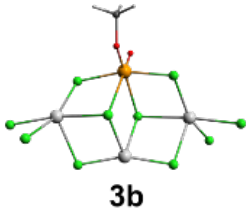

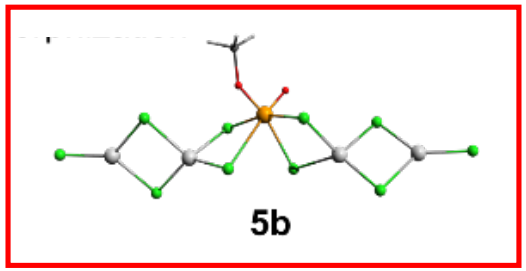

Effect of Geometry

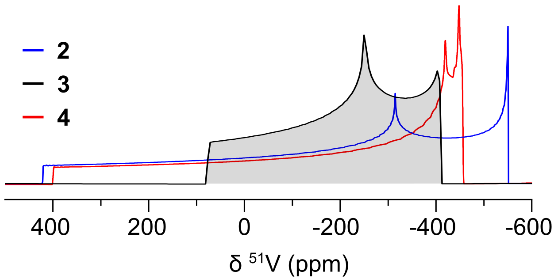

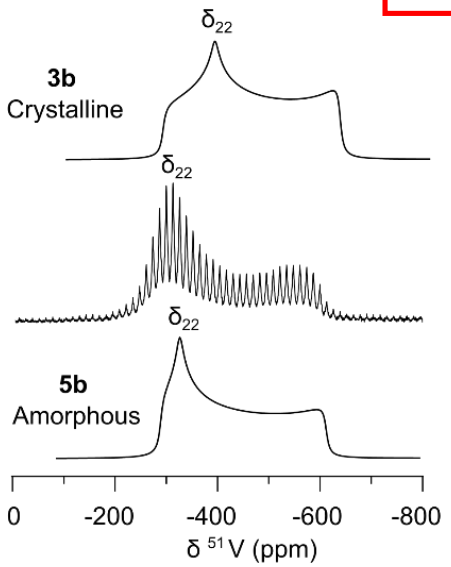

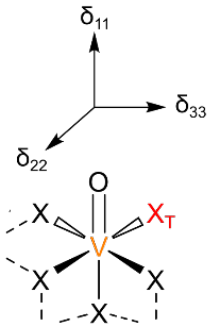

Effect of Anionic Ligands

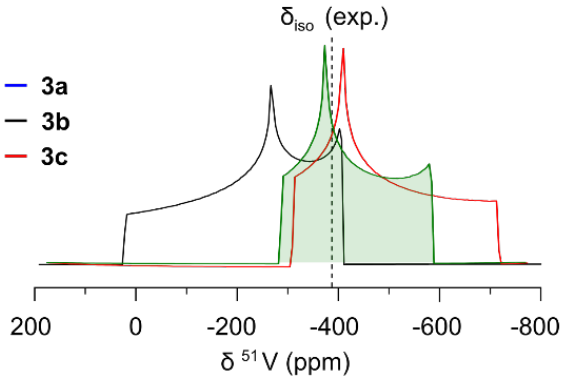

S. Sabisch, Y. Kakiuchi, S. R. Docherty, A. V. Yakimov, CCH
J. Am. Chem. Soc. 2023, *145*, 25595–25603.

NMR beyond Numbers

Understanding Electronic Structure and Reactivity from NMR

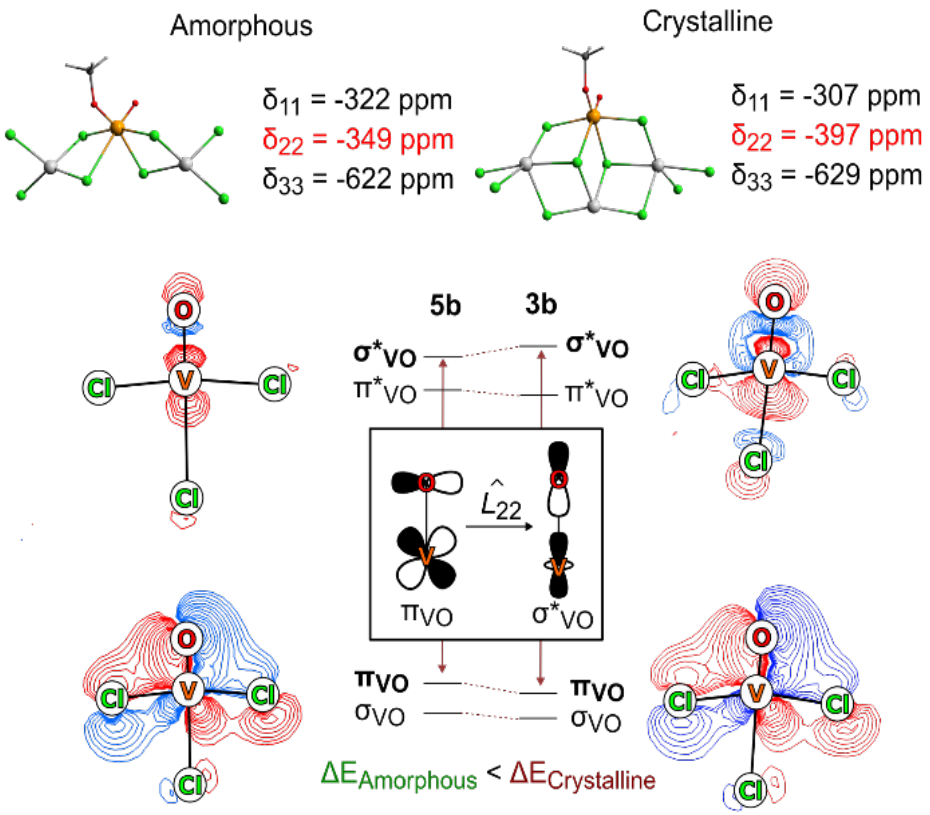

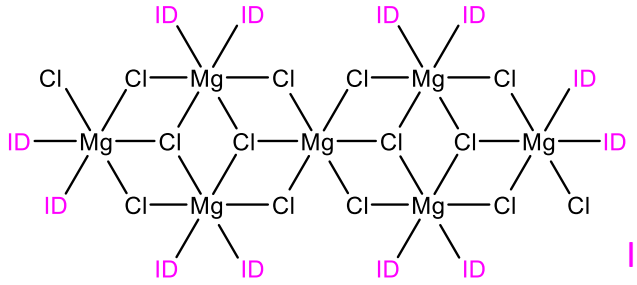

A complex Process yielding A Well-Defined Surface Species!

$VOCl_3$

Grafting & Amorphization

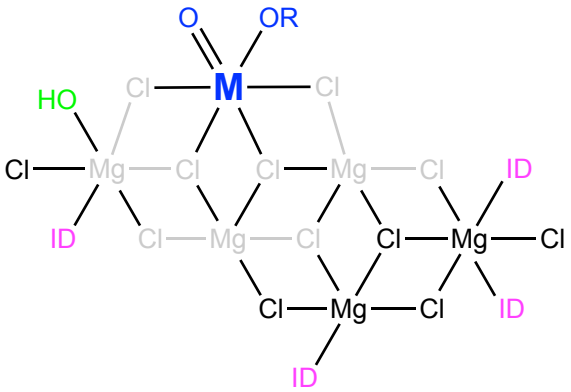

S. Sabisch, Y. Kakiuchi, S. R. Docherty, A. V. Yakimov, CCH
J. Am. Chem. Soc. 2023, *145*, 25595–25603.

NMR beyond Numbers

Understanding Electronic Structure and Reactivity from NMR

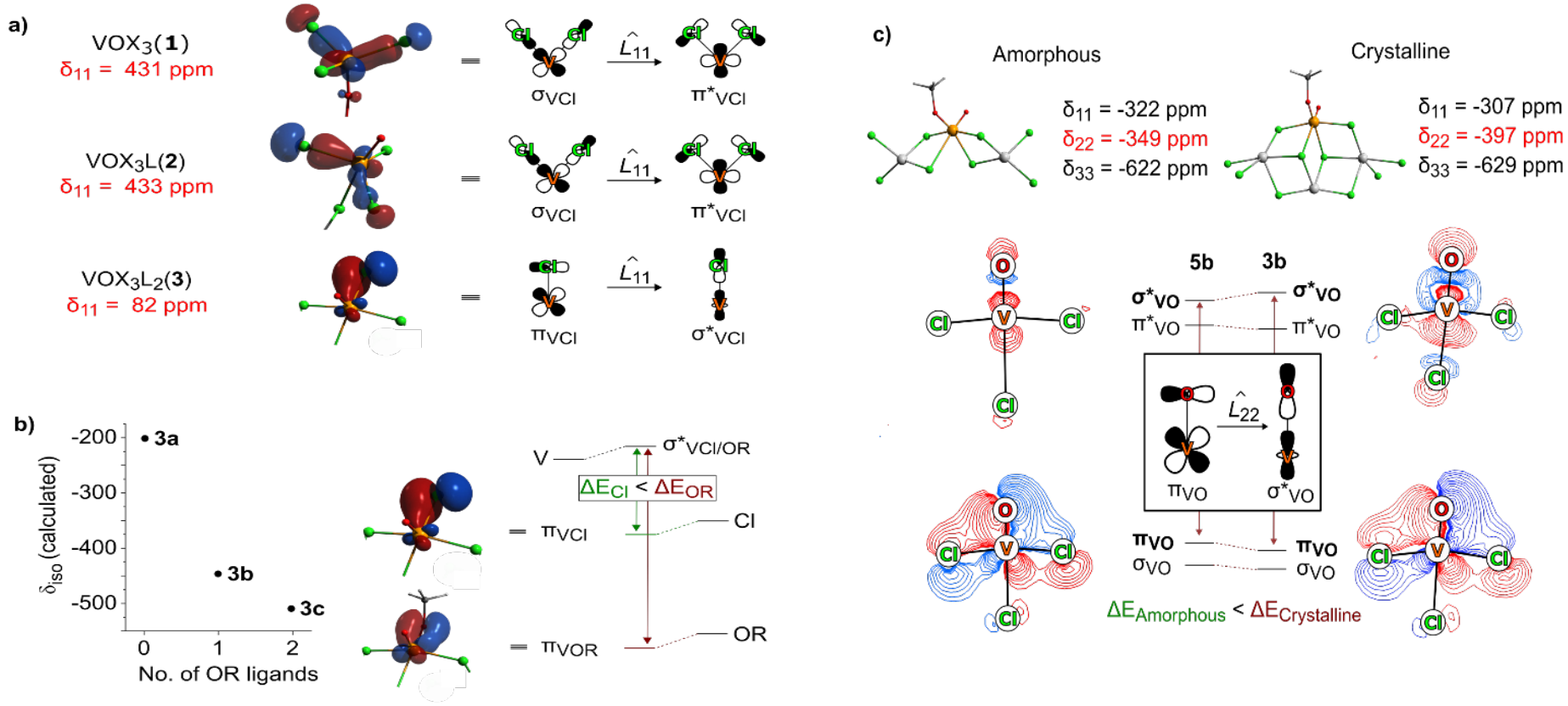

S. Sabisch, Y. Kakiuchi, S. R. Docherty, A. V. Yakimov, CCH
J. Am. Chem. Soc. 2023, *145*, 25595–25603.

NMR beyond Numbers

Understanding Electronic Structure and Reactivity from NMR

A case study:
Ziegler-Nata Catalysts

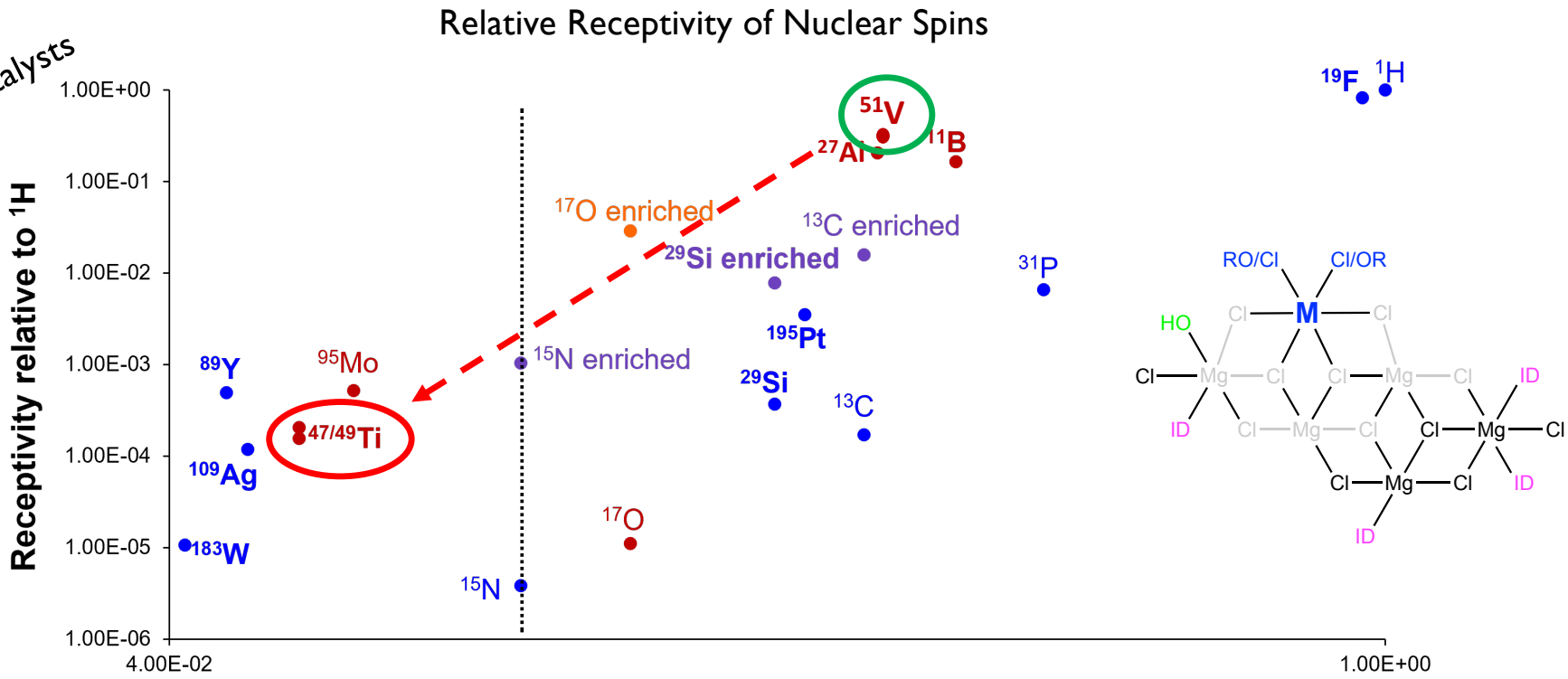

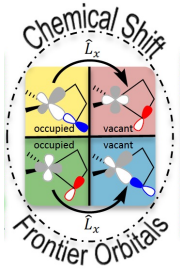

NMR beyond Numbers

Understanding Electronic Structure and Reactivity from NMR

Benchmark with Molecular Analogues

high-field NMR (900 MHz), Low Temperature (~100 K)
Magic Angle Spinning (10 kHz) and CPMG echo train acquisition

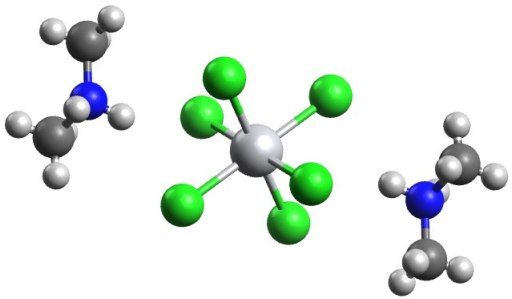

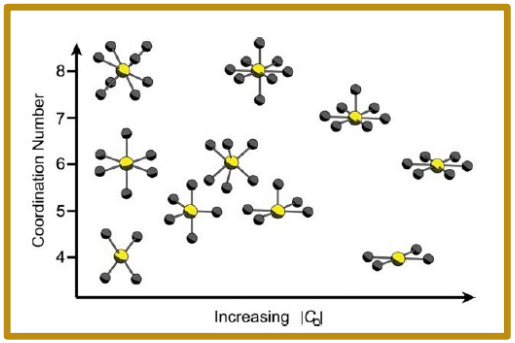

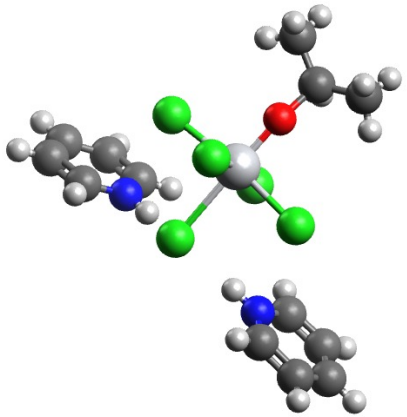

^{49}Ti

^{47}Ti

$\delta_{iso}(^{49}Ti) = -250$ ppm
$C_Q(^{49}Ti) = 3.0$ MHz

Low C_Q (DFT: 2.2 MHz)

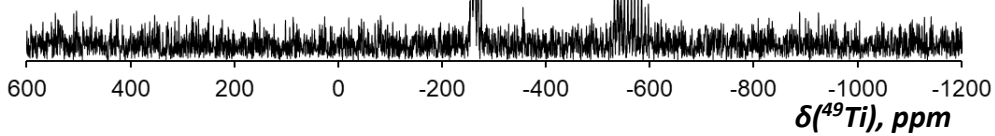

Asymmetry => Large C_Q (DFT: 22.9 MHz)

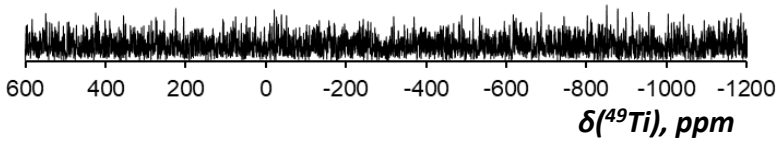

A. V. Yakimov, C. J. Kaul, Y. Kakiuchi, S. Sabisch, F. Morais Bolner, J. Raynaud, V. Monteil, P. Berruyer, C. Copéret J. Phys Chem. Lett. 2024, 15, 3178−3184

NMR beyond Numbers

Understanding Electronic Structure and Reactivity from NMR

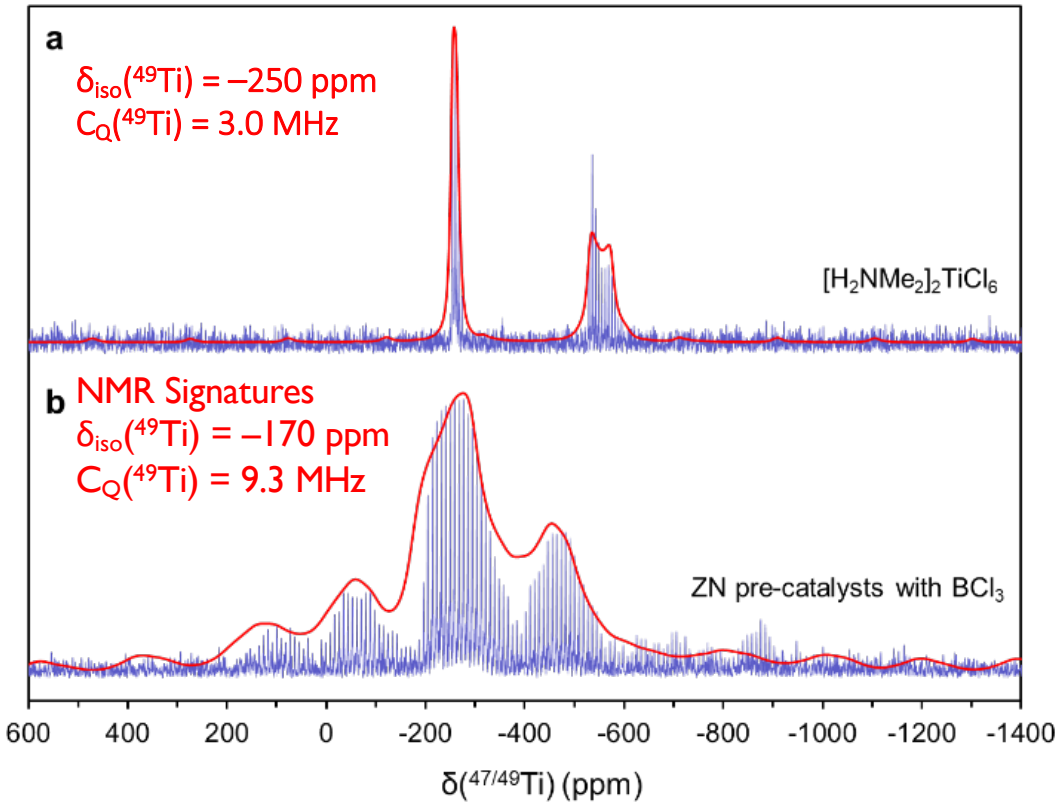

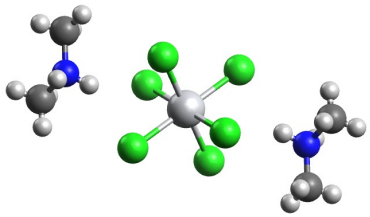

A molecular System

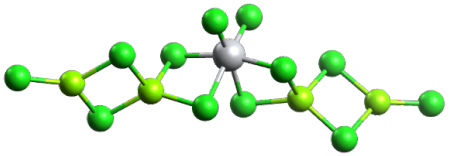

A well-defined Ti site

Thanks to L. Emsley
L. Piveteau (EPFL)

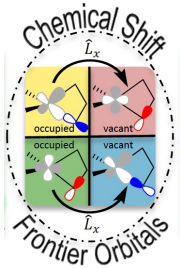

A. V. Yakimov, C. J. Kaul, Y. Kakiuchi, S. Sabisch, F. Morais Bolner, J. Raynaud, V. Monteil, P. Berruyer, C. Copéret J. Phys Chem. Lett. 2024, 15, 3178−3184

NMR beyond Numbers

Understanding Electronic Structure and Reactivity from NMR

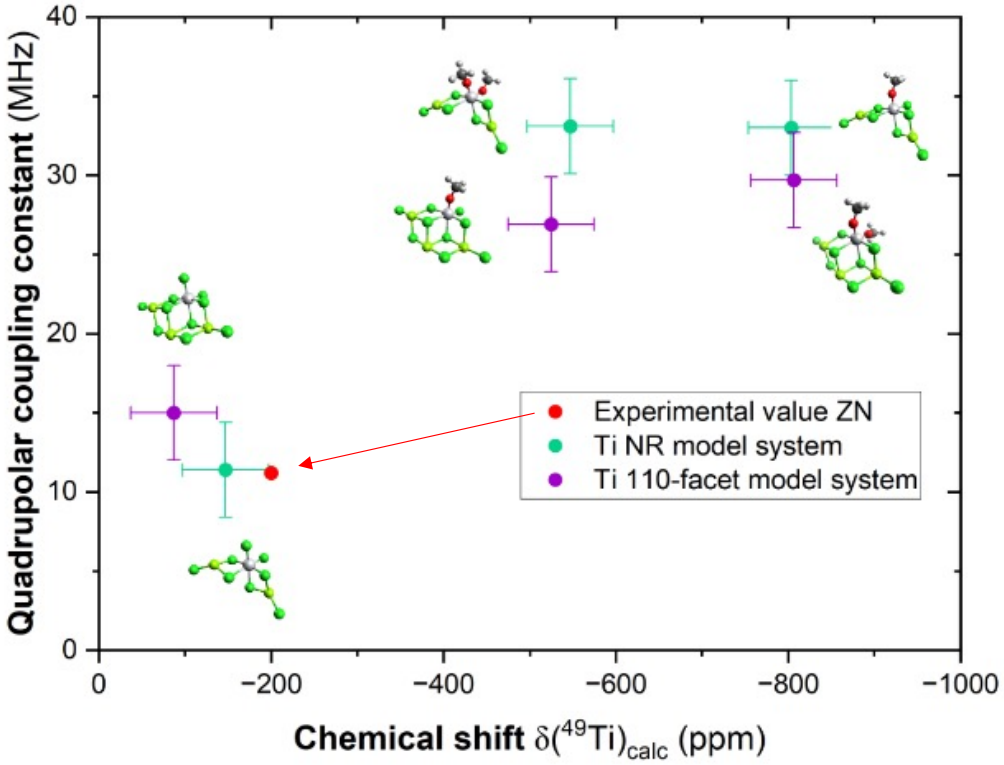

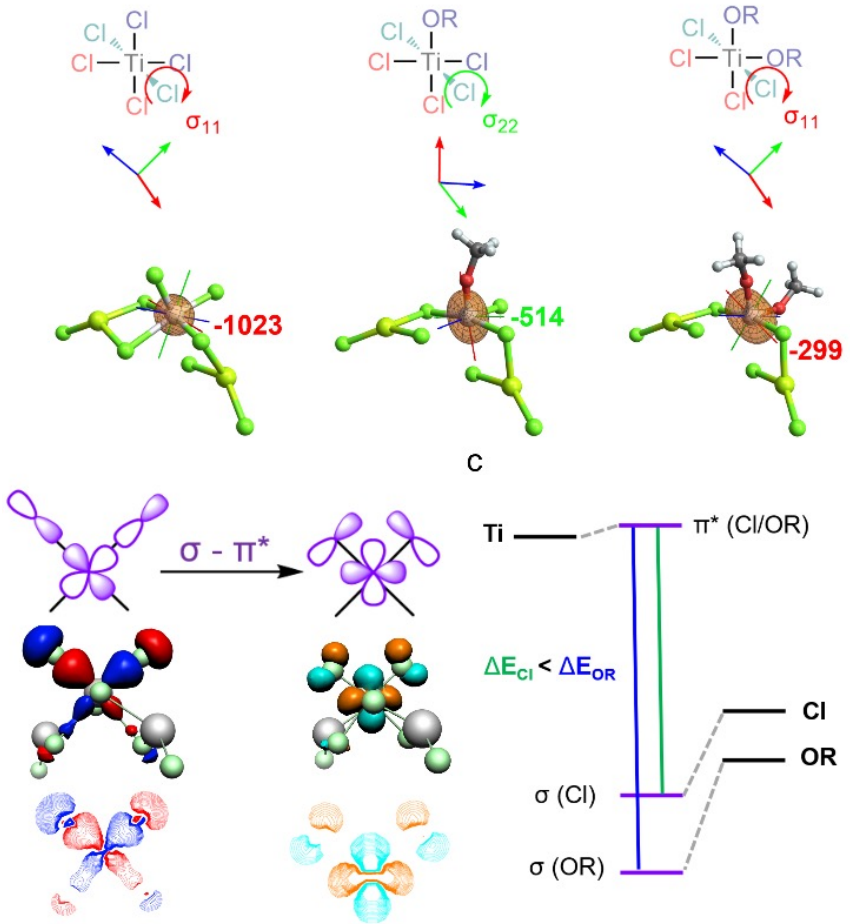

A. V. Yakimov, C. J. Kaul, Y. Kakiuchi, S. Sabisch, F. Morais Bolner, J. Raynaud, V. Monteil, P. Berruyer, C. Copéret J. Phys Chem. Lett. 2024, 15, 3178−3184

NMR beyond Numbers

Understanding Electronic Structure and Reactivity from NMR

Ziegler-Natta Pre-Catalysts

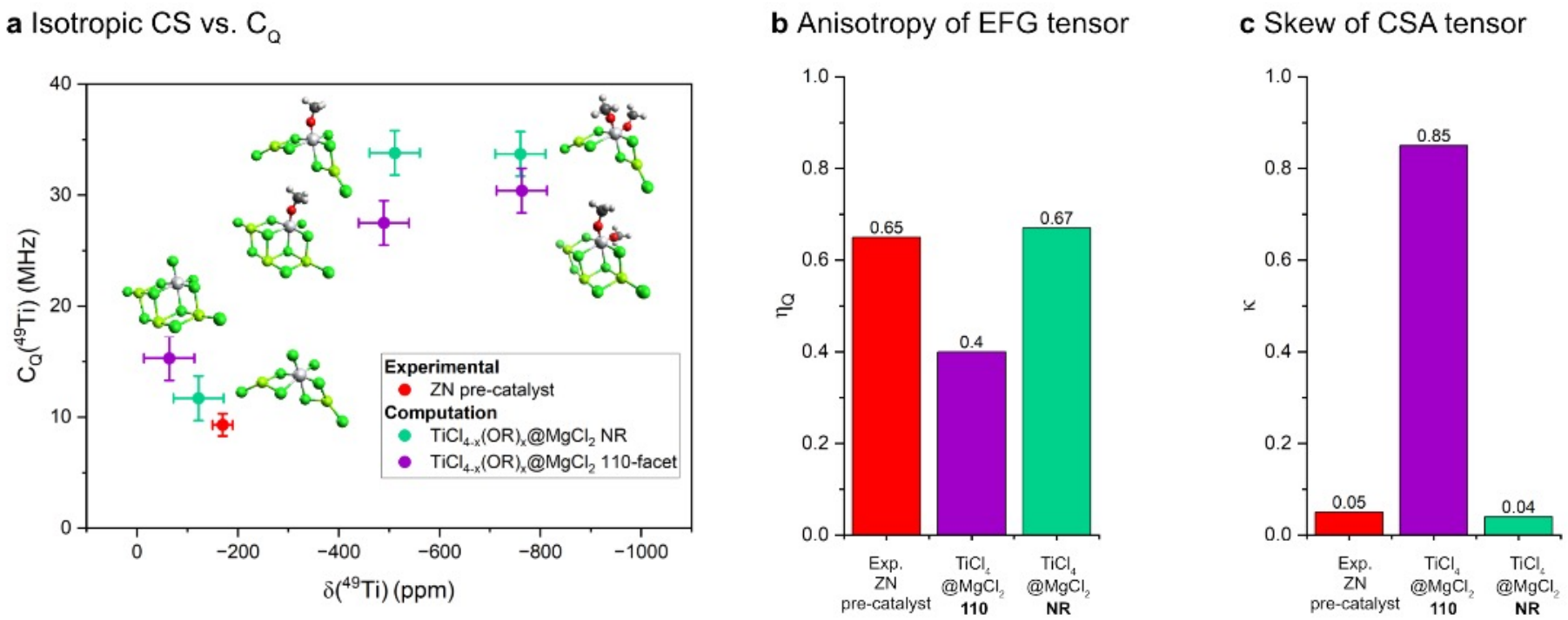

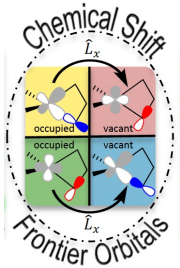

A. V. Yakimov, C. J. Kaul, Y. Kakiuchi, S. Sabisch, F. Morais Bolner, J. Raynaud, V. Monteil, P. Berruyer, C. Copéret J. Phys Chem. Lett. 2024, 15, 3178−3184

NMR beyond Numbers

Understanding Electronic Structure and Reactivity from NMR

A case study:
Ziegler-Nata Catalysts

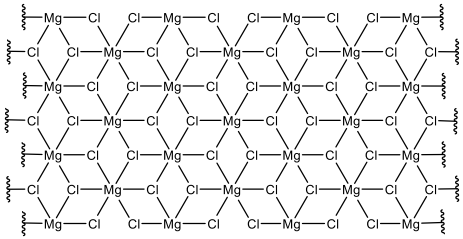

ID

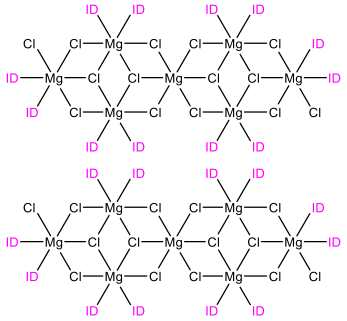

$TiCl_4$

Crystalline α(β)-$MgCl_2$

$MgCl_2$-ID nanoclusters

$TiCl_4$

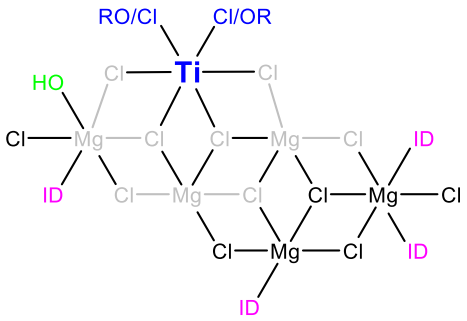

BCl_3

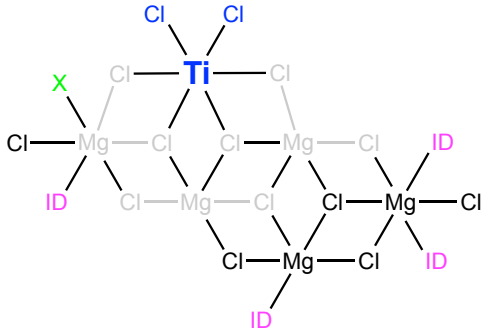

AlR_3/ED

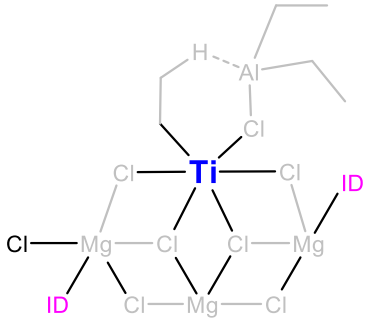

ZN pre-catalysts ***Modified ZN pre-catalysts*** ***Activated ZN catalyst***

Surface metal sites? Relation to active sites? Efficiency of Activation?

NMR beyond Numbers

Understanding Electronic Structure and Reactivity from NMR

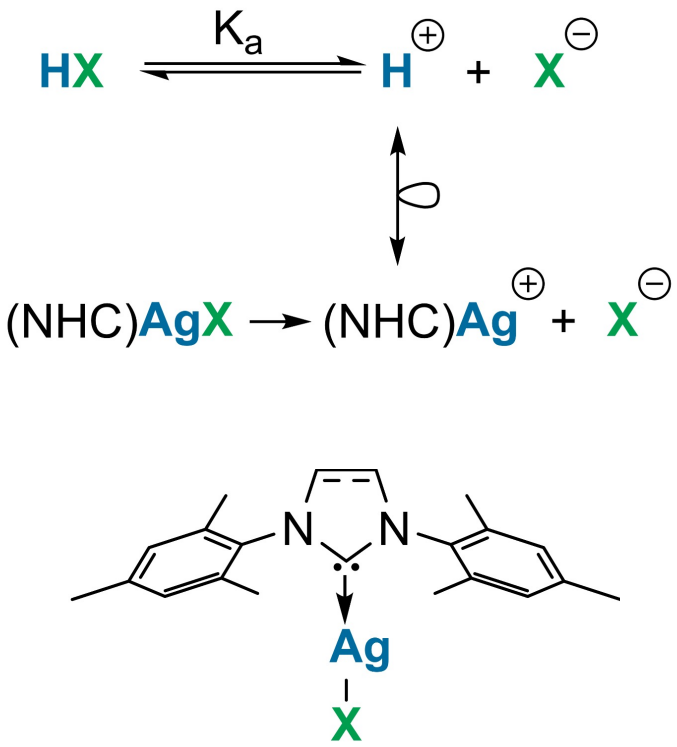

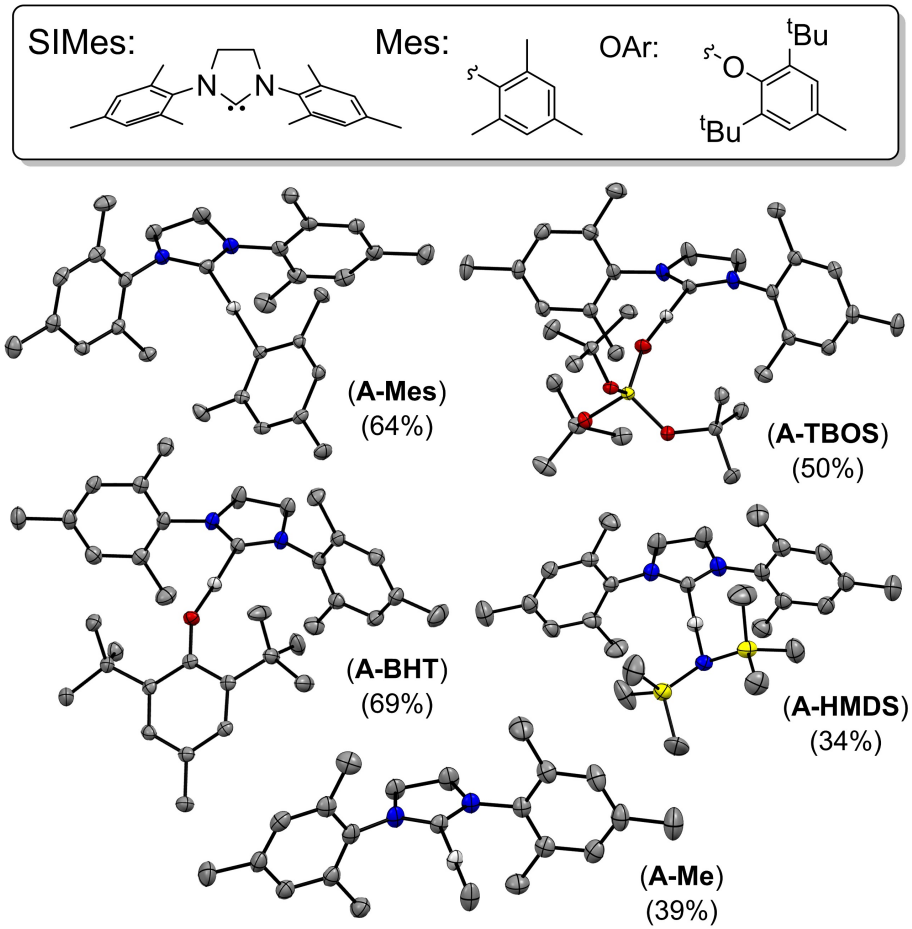

C. Hansen, S. R. Docherty, W. Cao, A. V. Yakimov, C. Copéret, Chem. Sci 2024, DOI: 10.1039/D3SC04067D

NMR beyond Numbers

Understanding Electronic Structure and Reactivity from NMR

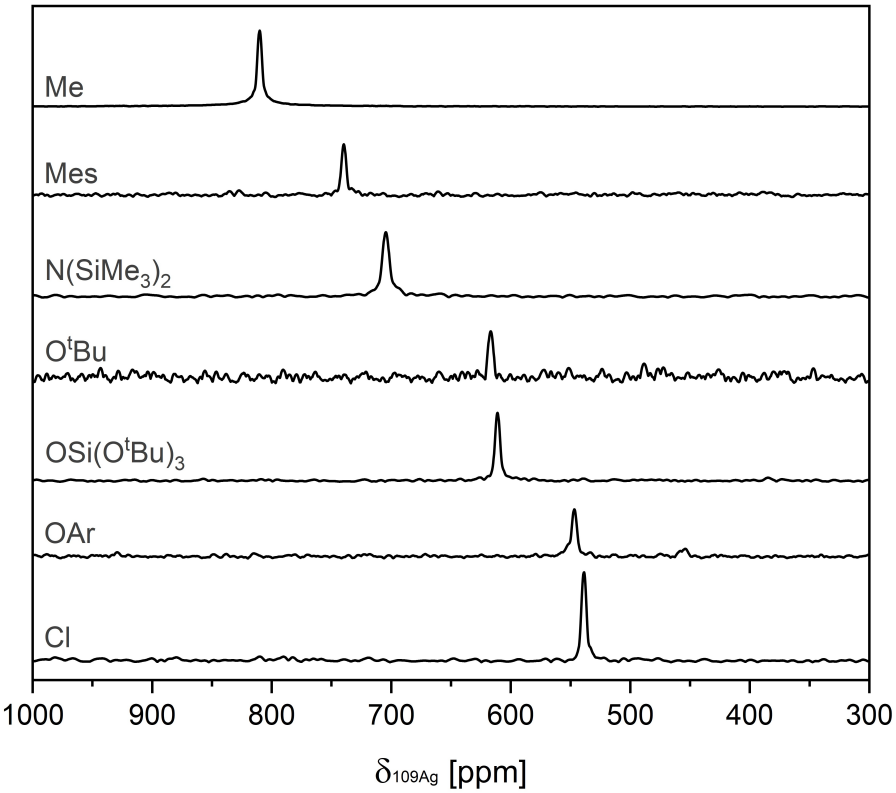

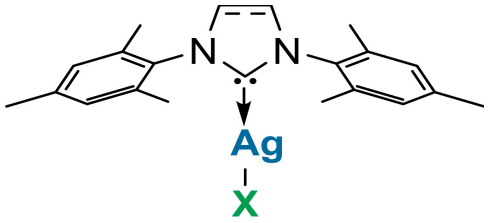

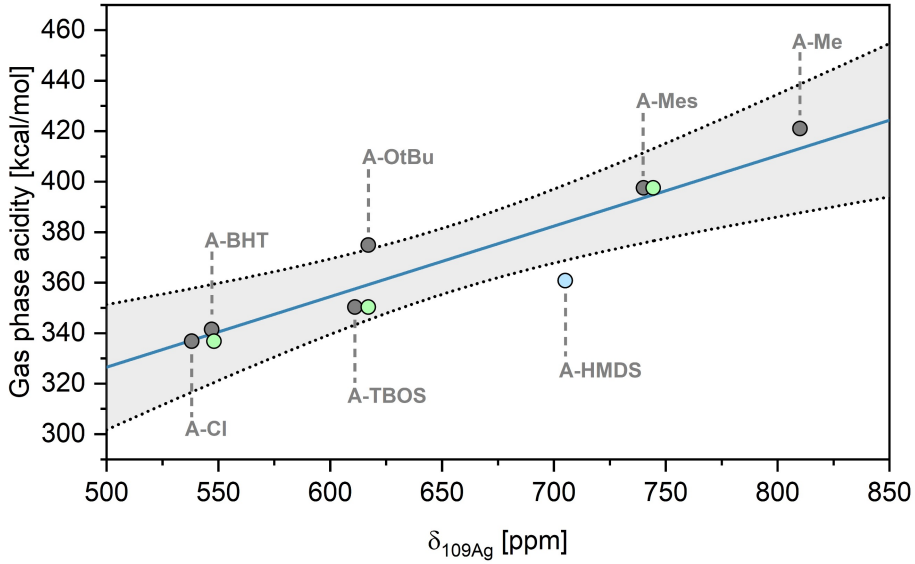

Linear correlation between DPE (pKa) and δ_{Ag} (solution or solid-state)

C. Hansen, S. R. Docherty, W. Cao, A. V. Yakimov, C. Copéret, *Chem. Sci* 2024, DOI: 10.1039/D3SC04067D

NMR beyond Numbers

Understanding Electronic Structure and Reactivity from NMR

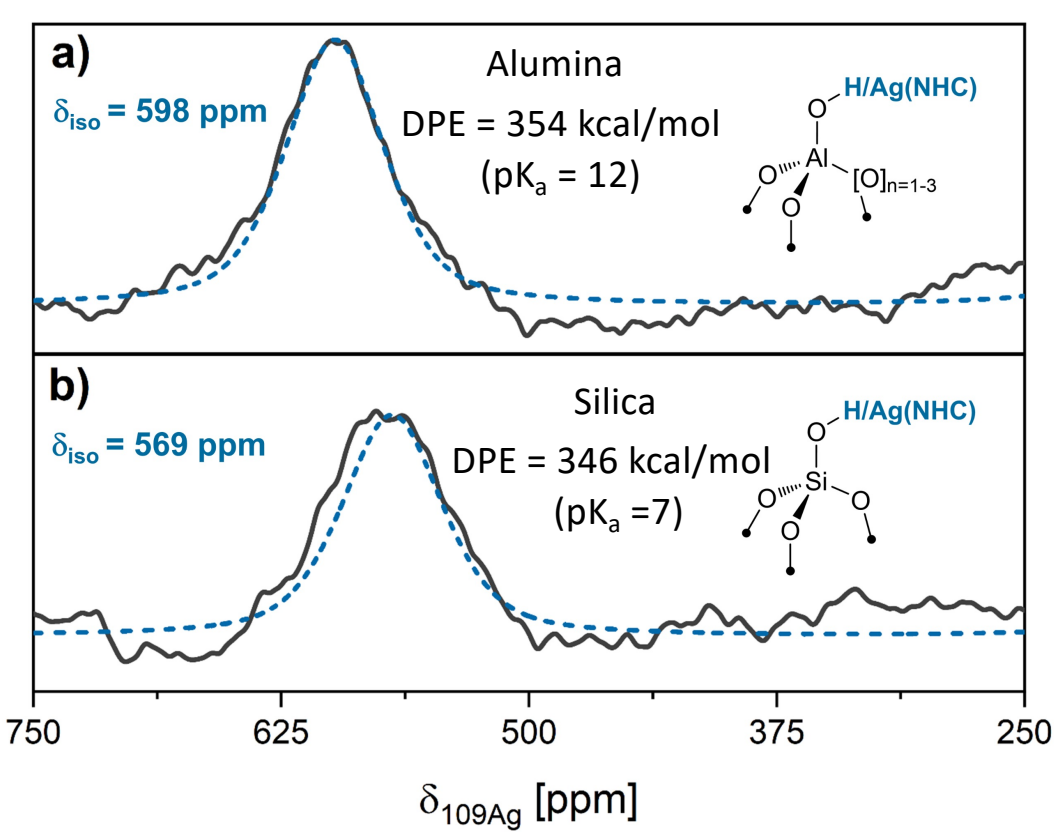

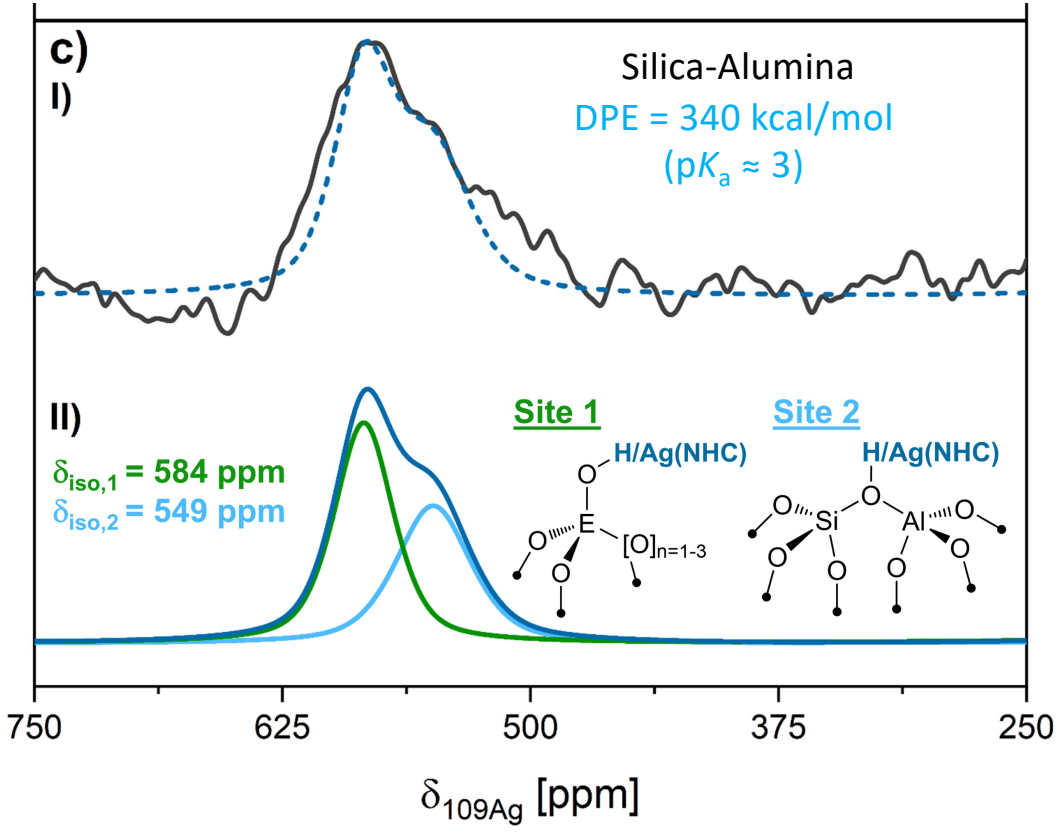

C. Hansen, S. R. Docherty, W. Cao, A. V. Yakimov, C. Copéret, Chem. Sci 2024, DOI: 10.1039/D3SC04067D

NMR beyond Numbers

Understanding Electronic Structure and Reactivity from NMR – Conclusion

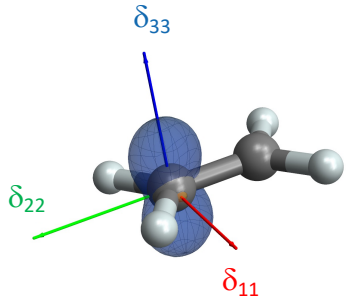

Solid-State NMR Spectroscopy – Chemical Shift Anisotropy

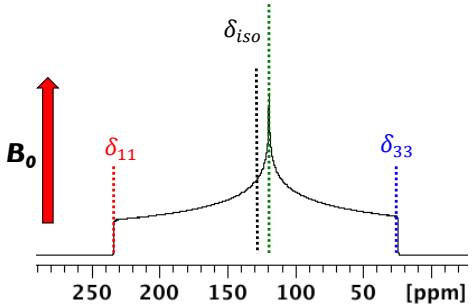

$$\sigma = \sigma_{dia} + \sigma_{para+SO}$$

$$\sigma_{ii,para} \Leftrightarrow \frac{\langle \Psi_{vac}|\hat{L}_i|\Psi_{occ}\rangle\langle \Psi_{vac}|\hat{L}_i/r^3|\Psi_{occ}\rangle}{\Delta E_{vac-occ}}$$

A Unique Operator for Spectroscopy

$$\hat{L}_i \Leftrightarrow \hat{R}_i$$

connecting
σ- and π-symmetry orbitals,
orthogonal to each other
with magnitude related to
Electronegativity difference,
hence reactivity

Frontier
Molecular Orbitals

Reactivity

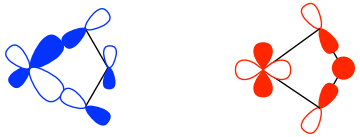

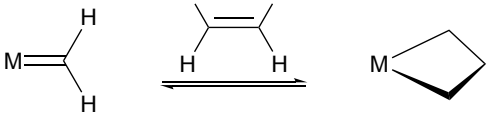

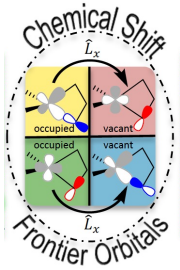

C. P. Gordon, L. Lätsch, CCH J. Phys. Chem. Lett. 2021, 12, 2072 (Perspectives).
C. P. Gordon, R. A. Andersen, CCH *Helvetica Chim Acta* 2019, 102, e1900151 (Tutorial)